

Contents lists available at ScienceDirect

# **Automatica**

journal homepage: www.elsevier.com/locate/automatica



# Global exponential stabilization of $2 \times 2$ linear hyperbolic PDEs via dynamic event-triggered backstepping control\*



Bhathiya Rathnayake a,\*, Mamadou Diagne b

- <sup>a</sup> Department of Electrical and Computer Engineering, University of California, San Diego, La Jolla, CA 92093, USA
- <sup>b</sup> Department of Mechanical and Aerospace Engineering, University of California, San Diego, La Jolla, CA 92093, USA

#### ARTICLE INFO

Article history: Received 13 October 2024 Received in revised form 16 April 2025 Accepted 5 August 2025

Keywords:
PDE backstepping
Event-triggered control
Periodic event-triggered control
Self-triggered control
Global exponential stability
Dynamic event-triggering

#### ABSTRACT

This paper introduces novel dynamic event-triggered control (ETC) mechanisms for 2 × 2 linear hyperbolic PDEs in three configurations: continuous-time event-triggered control (CETC), periodic event-triggered control (PETC), and self-triggered control (STC). These mechanisms ensure global exponential stability (GES) under ETC using PDE backstepping, with stability estimates provided in the spatial  $L^2$  norm of the states. The proposed CETC and PETC designs are observer-based and require continuous boundary measurements collocated with the actuation. In contrast, the STC design requires full-state measurements; however, unlike CETC and PETC, it does not require continuous measurements for the triggering mechanism-only measurements taken at event times. In the CETC design, a lower bound on the time between two consecutive events is enforced, and a dynamic variable with appropriately designed switching dynamics is introduced. By employing a novel Lyapunov functional, GES of the closed-loop system is established under zero-order hold implementation of the backstepping control between events. Events are triggered when the dynamic variable crosses zero from the positive side, after which it is immediately reset to an appropriate nonnegative value. Detecting events, therefore, necessitates continuous monitoring of this dynamic variable. To address this limitation, PETC and STC strategies are proposed. The PETC design identifies a suitable triggering condition that requires only periodic checks and derives an upper bound on the allowable sampling period. This PETC approach preserves the GES guaranteed by CETC without requiring continuous monitoring of a triggering condition, although it still relies on continuous measurements. Unlike CETC and PETC, STC requires neither continuous measurements nor monitoring of a triggering condition. Instead, at each event, STC computes the time to the next event — beyond a suitably enforced minimal dwell-time - using only measurements taken at events. Despite relying solely on event-triggered measurements, STC is capable of guaranteeing GES of the closed-loop system. The well-posedness of the closed-loop systems under all three strategies is established. A simulation study is provided to illustrate the theoretical results.

© 2025 Published by Elsevier Ltd.

# 1. Introduction

# 1.1. State of the art

Event-triggered control (ETC) of PDEs has gained traction due to the rise of networked control systems, which require efficient use of resources for communication, computation, and actuation. Two classes of event-triggering mechanisms are identified

E-mail addresses: brm222@ucsd.edu (B. Rathnayake), mdiagne@ucsd.edu (M. Diagne).

in ETC of PDEs: static event-triggering (Baudouin, Marx, & Tarbouriech, 2019; Diagne & Karafyllis, 2021; Espitia, Girard, Marchand, & Prieur, 2016; Espitia, Karafyllis, & Krstic, 2021; Kang, Baudouin, & Fridman, 2021; Koga, Demir, & Krstic, 2023; Koudohode, Baudouin, & Tarbouriech, 2022b; Koudohode, Espitia, & Krstic, 2024; Rathnayake & Diagne, 2022; Selivanov & Fridman, 2016) and dynamic event-triggering (Demir, Koga, & Krstic, 2024; Espitia, 2020; Espitia, Auriol, Yu, & Krstic, 2022a, 2022b; Espitia, Yu, & Krstic, 2020; Kang, Fridman, Zhang, & Liu, 2023; Katz, Fridman, & Selivanov, 2021; Koudohode, Baudouin, & Tarbouriech, 2022a; Lhachemi, 2024; Rathnayake & Diagne, 2024a; Rathnayake, Diagne, Cortés, & Krstic, 2025; Rathnayake, Diagne, Espitia, & Karafyllis, 2022; Rathnayake, Diagne, & Karafyllis, 2022; Wang & Krstic, 2021, 2022a, 2022b, 2022c, 2023; Zhang, Rathnayake, Diagne, & Krstic, 2025; Zhang & Yu, 2024). In static

This work was funded by the NSF CAREER Award CMMI-2302030 and the NSF grant CMMI-2222250. The material in this paper was not presented at any conference. This paper was recommended for publication in revised form by Associate Editor Rafael Vazquez under the direction of Editor Miroslav Krstic.

<sup>\*</sup> Corresponding author.

event-triggering, events are triggered based on a static rule, typically requiring full-state measurements, with a few exceptions, such as Espitia et al. (2016), Selivanov and Fridman (2016), where the designs can operate with outputs, though not with state estimates derived from observers. In contrast, dynamic eventtriggering utilizes a dynamic variable that has user-defined dynamics. This method can often be used with either full-state measurements or state estimates derived from observers. The greater flexibility offered by dynamic event-triggering arises from the auxiliary dynamics at the designer's disposal. Regarding the underlying controller, the most common approach is to implement a pre-designed continuous-time controller in a zero-order hold manner between control updates, a strategy known as control by emulation. PDE backstepping (Krstic & Smyshlyaev, 2008) and modal decomposition technique (Triggiani, 1980) are among the widely emulated continuous-time control approaches in PDE ETC. A key concern in ETC is avoiding Zeno behavior-the occurrence of an infinite number of control updates in a finite time interval, which leads to infeasible designs. A common way to ensure Zeno-freeness is to demonstrate or enforce a positive and uniform lower bound on the time between two consecutive events, referred to as the minimal dwell-time (MDT).

Previous studies on ETC of parabolic PDEs include works such as Demir, Koga, and Krstic (2024), Espitia et al. (2021), Kang et al. (2023), Katz et al. (2021), Koga et al. (2023), Koudohode et al. (2024), Lhachemi (2024), Rathnayake and Diagne (2022, 2024a), Rathnayake, Diagne, Espitia, and Karafyllis (2022), Rathnayake, Diagne, and Karafyllis (2022), Wang and Krstic (2023). Full-state feedback static event-triggering mechanisms for reaction-diffusion (RD) PDEs using PDE backstepping are proposed in Espitia et al. (2021). Koudohode et al. (2024), while dynamic event-triggering mechanisms are found in Rathnayake, Diagne, Espitia, and Karafyllis (2022), Rathnayake, Diagne, and Karafyllis (2022), Wang and Krstic (2023), with Wang and Krstic (2023) featuring a full-state feedback adaptive design and Rathnayake, Diagne, Espitia, and Karafyllis (2022), Rathnayake, Diagne, and Karafyllis (2022) being observer-based. Observer-based modal decomposition methods for dynamic ETC of RD PDEs are detailed in Katz et al. (2021), Lhachemi (2024). For parabolic PDEs with moving boundaries, static event-triggering using PDE backstepping is discussed in Koga et al. (2023), Rathnayake and Diagne (2022), requiring full-state measurements. Dynamic eventtriggering in the same context is presented in Demir, Koga, and Krstic (2024), Rathnayake and Diagne (2024a), with Demir, Koga, and Krstic (2024) proposing a full-state feedback design and Rathnayake and Diagne (2024a) an observer-based design. In Kang et al. (2023), the authors introduce a full-state feedback dynamic ETC method for nonlinear RD PDEs.

Previous works on ETC of hyperbolic PDEs include Baudouin et al. (2019), Diagne and Karafyllis (2021), Espitia (2020), Espitia et al. (2022a, 2022b, 2016, 2020), Koudohode et al. (2022b), Wang and Krstic (2021, 2022a, 2022b, 2022c), Zhang and Yu (2024). Static event-triggering is used in Baudouin et al. (2019), Diagne and Karafyllis (2021), Espitia et al. (2016), Koudohode et al. (2022b), addressing linear hyperbolic systems (Espitia et al., 2016), damped wave equations (Baudouin et al., 2019; Koudohode et al., 2022b), and nonlinear hyperbolic PDEs in manufacturing (Diagne & Karafyllis, 2021). Output feedback is used in Espitia et al. (2016), while full-state feedback is required in the others. Dynamic triggering, employed in Espitia (2020), Espitia et al. (2022a, 2022b, 2020), Wang and Krstic (2021, 2022a, 2022b, 2022c), Zhang and Yu (2024), focuses on  $2 \times 2$  linear hyperbolic PDEs (Espitia, 2020; Wang & Krstic, 2021, 2022a, 2022b, 2022c) and 4 × 4 systems (Espitia et al., 2022a, 2022b; Zhang & Yu, 2024). All use PDE backstepping, with full-state feedback in Espitia et al. (2020), Wang and Krstic (2022b), Zhang and Yu (2024) and observer-based feedback in the others.

One key limitation of the discussed ETC approaches is that they require continuous monitoring of conditions to detect events. Therefore, these mechanisms are referred to as continuous-time ETC (CETC) methods. As continuous monitoring on digital computers is impractical, two alternative methods have emerged: periodic event-triggered control (PETC), which periodically checks conditions (Demir, Diagne, & Krstic, 2024; Rathnayake & Diagne, 2023, 2024b; Rathnayake et al., 2025; Selivanov & Fridman, 2016; Somathilake, Rathnayake, & Diagne, 2024; Wakaiki & Sano, 2020; Zhang et al., 2025), and self-triggered control (STC), which predicts the next event time at the current event based on system states and dynamics (Rathnayake & Diagne, 2024b; Rathnayake et al., 2025; Somathilake et al., 2024; Wakaiki & Sano, 2019; Zhang et al., 2025). Works such as Selivanov and Fridman (2016). Wakaiki and Sano (2020) use periodic static event-triggering with full-state measurements for semilinear diffusion PDEs and linear infinite-dimensional systems. The full-state feedback STC method from Wakaiki and Sano (2019) targets linear infinite-dimensional systems. Dynamic periodic event-triggering and self-triggering with PDE backstepping are examined in Demir, Diagne, and Krstic (2024), Rathnayake and Diagne (2023, 2024b), Rathnayake et al. (2025). Somathilake et al. (2024), Zhang et al. (2025). These include observer-based PETC and STC approaches for RD PDEs (Rathnayake & Diagne, 2024b) and 2 × 2 linear hyperbolic PDEs (Somathilake et al., 2024), full-state feedback and observer-based PETC approaches for parabolic PDEs with moving boundaries (Demir, Diagne, & Krstic, 2024; Rathnayake & Diagne, 2023), and full-state feedback PETC and STC using performance barriers for sparser event-triggering in RD PDEs (Rathnayake et al., 2025) and  $2 \times 2$  linear hyperbolic PDEs (Zhang et al., 2025).

#### 1.2. Contributions

In this paper, we propose novel dynamic event-triggering mechanisms for  $2 \times 2$  linear hyperbolic PDEs with PDE backstepping in three configurations: CETC, PETC, and STC. These mechanisms achieve global exponential stability (GES) under eventtriggered PDE backstepping control—an outcome that, to the best of our knowledge, has not been previously realized using dynamic event-triggering. Previous works, such as Demir, Diagne, and Krstic (2024), Demir, Koga, and Krstic (2024), Espitia (2020), Espitia et al. (2022a, 2022b, 2020), Rathnayake and Diagne (2023, 2024a, 2024b), Rathnayake et al. (2025), Rathnayake, Diagne, Espitia, and Karafyllis (2022), Rathnayake, Diagne, and Karafyllis (2022), Somathilake et al. (2024), Wang and Krstic (2021, 2022a, 2022b, 2022c, 2023), Zhang et al. (2025), Zhang and Yu (2024), that have employed dynamic event-triggering for PDE backstepping, have only established (global) exponential convergence to equilibrium. In these works, demonstrating the existence of an MDT to rule out Zeno behavior while guaranteeing closedloop system exponential stability leads to conflicting conditions, allowing only the establishment of exponential convergence. In addition to the GES guaranteed by our proposed designs, the novel STC framework further advances the state of the art by requiring only event-triggered measurements for the triggering mechanism-a feature not yet achieved by either static (Espitia et al., 2021; Koga et al., 2023; Koudohode et al., 2024; Rathnayake & Diagne, 2022) or dynamic event-triggering (Demir, Diagne, & Krstic, 2024; Demir, Koga, & Krstic, 2024; Espitia, 2020; Espitia et al., 2022a, 2022b, 2020; Rathnayake & Diagne, 2023, 2024a, 2024b; Rathnayake et al., 2025; Rathnayake, Diagne, Espitia, &

<sup>&</sup>lt;sup>1</sup> Despite the claims of (G)ES in Demir, Koga, and Krstic (2024), Espitia (2020), Zhang and Yu (2024), and Theorem 3 of Espitia et al. (2020), these only guarantee (global) exponential convergence to the equilibrium.

**Table 1**Position of the current work within the state of the art in dynamic event-triggering for PDE backstepping control.

PDE type	Dynamic ETC with PDE backstepping	(G)ES	PETC	STC	Event-triggered measurements
Parabolic	Demir, Koga, and Krstic (2024), Rathnayake and Diagne (2024a), Rathnayake, Diagne, Espitia, and Karafyllis (2022), Rathnayake, Diagne, and Karafyllis (2022), Wang and Krstic (2023)	Х	Х	X	Х
	Demir, Diagne, and Krstic (2024), Rathnayake and Diagne (2023)	X	✓	X	X
	Rathnayake and Diagne (2024b), Rathnayake et al. (2025)	X	✓	✓	X
Hyperbolic	Espitia (2020), Espitia et al. (2022a, 2022b, 2020), Wang and Krstic (2021, 2022a, 2022b, 2022c), Zhang and Yu (2024)	Х	X	Х	Х
	Somathilake et al. (2024), Zhang et al. (2025)	X	✓	✓	X
	This work	GES ✓	✓	✓	✓

**Table 2** A comparison of the event-triggering mechanisms proposed in this work.

	Observer- based	Cont. check of trig. Cond. Not Required	Event-triggered Meas. only
CETC	✓	X	X
PETC	✓	✓	X
STC	X	$\checkmark$	✓

Karafyllis, 2022; Rathnayake, Diagne, & Karafyllis, 2022; Somathilake et al., 2024; Wang & Krstic, 2021, 2022a, 2022b, 2022c, 2023; Zhang et al., 2025; Zhang & Yu, 2024) strategies for PDE backstepping control, all of which require continuous measurements. Table 1 illustrates how this work fits within the current state of the art in dynamic event-triggering for PDE backstepping control.

Our CETC and PETC designs are observer-based, requiring continuous but only boundary measurements collocated with the actuation. Our STC design requires full-state measurements; however, unlike CETC and PETC, it does not require continuous measurements for the triggering mechanism, only measurements taken at events generated by the self-triggering mechanism. Both PETC and STC eliminate the drawback of CETC, which requires continuous monitoring of a triggering condition to detect events. PETC addresses this by checking an appropriate triggering condition periodically, while STC computes the next event time at the current event time using event-triggered measurements. Table 2 presents a qualitative comparison of the designs proposed in this work.

The design of the CETC approach involves explicitly enforcing a suitable lower bound,  $\tau > 0$ , on the time between two events, thereby ruling out Zeno behavior. This contrasts with (Demir, Koga, & Krstic, 2024; Espitia, 2020; Espitia et al., 2022a, 2022b, 2020; Rathnayake & Diagne, 2024a; Rathnayake et al., 2025; Rathnayake, Diagne, Espitia, & Karafyllis, 2022; Rathnayake, Diagne, & Karafyllis, 2022; Wang & Krstic, 2021, 2022a, 2022b, 2022c, 2023; Zhang et al., 2025; Zhang & Yu, 2024), where the existence of a minimum dwell-time is not explicitly evident from the triggering condition and requires proof of its existence. We introduce a switching dynamic variable that remains non-negative between the last event at time  $t_i$  and  $t_i + \tau$ , for  $j \in \mathbb{N}$ , and is allowed to decrease until the next event, which occurs at time  $t_{i+1}, j \in \mathbb{N}$  at the zero-crossing of the dynamic variable. The concept of time regularization to enforce an MDT and the use of a switching dynamic variable is not entirely novel in PDE ETC. For example, see Kang et al. (2023), Katz et al. (2021), where the authors propose dynamic ETC strategies for parabolic PDEs, using arguments involving linear matrix inequalities. However, our work is primarily inspired by Dolk and Heemels (2017), Dolk, Ploeg, and Heemels (2017), Dolk, Tesi, De Persis, and Heemels (2017), where dynamic ETC approaches are developed for networked control systems described by ordinary differential equations, employing switching dynamic variables. Drawing from these ideas, we construct a novel Lyapunov candidate for  $2 \times 2$  linear hyperbolic PDEs under ETC. This candidate includes the  $L^2$  norms of the observer and observer error target system states, the switching dynamic variable, and a state-independent dynamic reset variable that is modulated by the control input sampling error. Through a careful choice of the switching dynamics, its initial conditions at each event, and an appropriate MDT  $\tau>0$  derived from the state-independent dynamic reset variable, we establish that the Lyapunov function remains dissipative along the closed-loop system dynamics despite the event-triggered application of the control input with zero-order hold. This allows us to establish, for the first time, GES under PDE backstepping with dynamic event-triggering. The zero-crossing of the switching dynamic variable must be monitored continuously in time to detect events, hence the name CETC. The proposed PETC and STC designs overcome this drawback.

The design of the PETC approach involves: (1) identifying an appropriate triggering condition that requires only periodic checks to determine if control updates are necessary, and (2) determining an appropriate upper bound for the allowable sampling period for periodic checks. Building on the ideas from (Rathnayake & Diagne, 2024b), a novel event-triggering function for PETC is derived by finding an upper bound for the underlying continuous-time event-triggering function. Its derivation necessitates establishing a sufficiently small upper bound for the sampling period of the triggering mechanism. Despite the triggering function being evaluated only periodically, as opposed to the continuous monitoring required in CETC, the PETC mechanism preserves the GES guaranteed by CETC. Since the triggering condition is checked periodically, Zeno behavior is inherently absent.

Unlike the proposed CETC and PETC mechanisms, the proposed STC does not require monitoring any triggering conditions. The STC triggering mechanism is designed by (1) enforcing an MDT  $\tau$  > 0, similar to CETC, and (2) identifying an appropriate waiting time until the next event at time  $t_{i+1}$ , starting from  $t_i$  +  $\tau$  for  $j \in \mathbb{N}$ , using event-triggered measurements only. This waiting time is derived by utilizing suitable upper bounds on the system states between events and employing a switching dynamic variable similar to that in CETC. GES under STC is then established using Lyapunov arguments akin to those in CETC. In contrast to CETC, PETC, and previous ETC designs employing static event-triggering (Espitia et al., 2021; Koga et al., 2023; Koudohode et al., 2024; Rathnayake & Diagne, 2022) or dynamic event-triggering (Demir, Diagne, & Krstic, 2024; Demir, Koga, & Krstic, 2024; Espitia, 2020; Espitia et al., 2022a, 2022b, 2020; Rathnayake & Diagne, 2023, 2024a, 2024b; Rathnayake et al., 2025; Rathnayake, Diagne, Espitia, & Karafyllis, 2022; Rathnayake, Diagne, & Karafyllis, 2022; Somathilake et al., 2024; Wang & Krstic, 2021, 2022a, 2022b, 2022c, 2023; Zhang et al., 2025; Zhang & Yu, 2024), all of which require continuous measurements for their triggering mechanisms (see Table 1), the proposed STC design relies solely on event-triggered measurements – specifically, the measurements at the current event time  $t_i$  and the previous event time  $t_{i-1}$  — to determine the next event time  $t_{i+1}$ ,  $j \in \mathbb{N}$ .

The well-posedness of the closed-loop system under all three ETC approaches is obtained.

#### **Contributions Summary**

- 1. The design of a novel observer-based CETC for 2 × 2 linear hyperbolic PDEs that guarantees GES. To the best of our knowledge, this is the first approach to achieve GES for hyperbolic PDEs under dynamic ETC with PDE backstepping. Previous works such as Demir, Koga, and Krstic (2024), Espitia (2020), Espitia et al. (2022a, 2022b, 2020), Rathnayake and Diagne (2024a), Rathnayake et al. (2025), Rathnayake, Diagne, Espitia, and Karafyllis (2022), Rathnayake, Diagne, and Karafyllis (2022), Wang and Krstic (2021, 2022a, 2022b, 2022c, 2023), Zhang et al. (2025), Zhang and Yu (2024), which employ PDE backstepping with dynamic event-triggering, have only established (global) exponential convergence.
- 2. The design of a novel observer-based PETC for 2 × 2 linear hyperbolic PDEs that guarantees GES. PETC eliminates the need for continuous checking of a triggering condition required in CETC, requiring only periodic checks of a suitable triggering condition. This is the first PETC design with PDE backstepping that guarantees GES. Previous PETC approaches using PDE backstepping such as Demir, Diagne, and Krstic (2024), Rathnayake and Diagne (2023, 2024b), Rathnayake et al. (2025), Somathilake et al. (2024), Zhang et al. (2025) have only established (global) exponential convergence.
- 3. The design of a novel full-state feedback STC for  $2 \times 2$  linear hyperbolic PDEs that guarantees GES and requires only event-triggered measurements for the triggering mechanism. STC eliminates the need for continuous monitoring of a triggering function required in CETC, and instead calculates the next event time at each event using eventtriggered measurements. This is the first STC design with PDE backstepping that guarantees GES. Previous STC approaches using PDE backstepping, such as Rathnayake and Diagne (2024b), Rathnayake et al. (2025), Somathilake et al. (2024), Zhang et al. (2025), have only established (global) exponential convergence. Furthermore, this is the first ETC design with PDE backstepping that requires only eventtriggered measurements for the triggering mechanism. Previous works on ETC with PDE backstepping using either static (Espitia et al., 2021; Koga et al., 2023; Koudohode et al., 2024; Rathnayake & Diagne, 2022) or dynamic eventtriggering (Demir, Diagne, & Krstic, 2024; Demir, Koga, & Krstic, 2024; Espitia, 2020; Espitia et al., 2022a, 2022b, 2020; Rathnayake & Diagne, 2023, 2024a, 2024b; Rathnayake et al., 2025; Rathnayake, Diagne, Espitia, & Karafyllis, 2022; Rathnayake, Diagne, & Karafyllis, 2022; Somathilake et al., 2024; Wang & Krstic, 2021, 2022a, 2022b, 2022c, 2023; Zhang et al., 2025; Zhang & Yu, 2024) require continuous measurements for the triggering mechanism.

#### 1.3. Organization

The paper is organized as follows. In Section 2, we present the continuous-time control and its emulation. Sections 3, 4, and 5 present the CETC, PETC, and STC designs, respectively. A simulation study is conducted in Section 6 to illustrate the results, and conclusions are provided in Section 7.

#### 1.4. Notations

Let  $\mathbb R$  be the set of real numbers,  $\mathbb R_{>0}$  be the set of positive real numbers, and  $\mathbb R_{\geq 0}$  be the set of nonnegative real numbers

including zero. Let  $\mathbb{N}$  be the set of natural numbers including 0, and let  $\mathbb{N}_{>0}$  be the set of natural numbers greater than 0. By  $L^2(0,1)$ , we denote the equivalence class of Lebesgue measurable functions  $f:[0,1]\to\mathbb{R}$  such that  $\|f\|_{L^2((0,1);\mathbb{R})}=(\int_0^1|f(x)|^2)^{1/2}<\infty$ . Define  $\mathcal{C}^0(I;L^2((0,1);\mathbb{R}))$  as the space of continuous functions  $u(\cdot,t)$  for an interval  $I\subseteq\mathbb{R}_{>0}$  such that  $I\ni t\to u(\cdot,t)\in L^2((0,1);\mathbb{R})$ .

## 2. Preliminaries and problem formulation

Consider the following  $2 \times 2$  linear hyperbolic PDE system in the canonical form:

$$u_t(x,t) + \lambda_1 u_x(x,t) = c_1(x)v(x,t), \ \forall x \in (0,1),$$
 (1)

$$v_t(x,t) - \lambda_2 v_x(x,t) = c_2(x)u(x,t), \ \forall x \in (0,1),$$
 (2)

with boundary conditions

$$u(0,t) = qv(0,t),$$
 (3)

$$v(1,t) = \rho u(1,t) + U_i. \tag{4}$$

for all  $t \in (t_j, t_{j+1}), j \in \mathbb{N}$ . The set  $\{t_j\}_{j \in \mathbb{N}}$  represents the sequence of control update times, which will later be characterized under continuous-time event-triggered control (CETC), periodic event-triggered control (PETC), and self-triggered control (STC) strategies. The control input  $U_j$  remains constant for all  $t \in [t_j, t_{j+1})$ , where  $j \in \mathbb{N}$ . The parameters  $\lambda_1, \lambda_2 > 0$  denote the transport speeds, while the functions  $c_1(x)$  and  $c_2(x)$  are such that  $c_1, c_2 \in C^0((0, 1); \mathbb{R})$ . The parameter  $q \neq 0$  represents the distal reflection term, and  $\rho$  is the proximal reflection term. The initial conditions are given by  $(u^0, v^0)^T \in L^2((0, 1); \mathbb{R}^2)$ .

We make the following assumption on the reflection terms.

**Assumption 1.** The reflection terms are small enough such that the following inequality holds:

$$|\rho q| < \frac{1}{\sqrt{3}}.\tag{5}$$

**Remark 1.** By performing a spectrum analysis similar to Yu and Krstic (2022) for the system (1)–(4), with  $c_1(x) \equiv c_1$  and  $c_2(x) \equiv c_2$ , and with  $U_j = 0$  (open-loop system), one can show that a sufficient condition for instability is

$$4c_1c_2 > (\lambda_1 + \lambda_2)^2 \xi_1^2, \tag{6}$$

where  $\xi_1 > 0$  is the smallest admissible spatial frequency determined by the boundary conditions. Assumption 1 imposes dissipative boundary conditions, which do not contribute to instability. However, in the presence of in-domain couplings between the two transport PDEs (1) and (2), the condition (6) ensures that at least one eigenvalue has a positive real part, leading to instability.

In Vazquez, Krstic, and Coron (2011), among other results, the authors develop an observer for the system (1)–(4) using u(1,t) as the available boundary measurement, resulting in a collocated sensing and actuation setup. This design is presented below. The observer states  $(\hat{u}, \hat{v})$  satisfy for all  $x \in (0, 1)$ 

$$\hat{u}_t(x,t) + \lambda_1 \hat{u}_x(x,t) = c_1(x)\hat{v}(x,t) + p_1(x)\tilde{u}(1,t), \tag{7}$$

$$\hat{v}_t(x,t) - \lambda_2 \hat{v}_x(x,t) = c_2(x)\hat{u}(x,t) + p_2(x)\tilde{u}(1,t), \tag{8}$$

with boundary conditions

$$\hat{u}(0,t) = q\hat{v}(0,t),$$
 (9)

$$\hat{v}(1,t) = \rho u(1,t) + U_i, \tag{10}$$

for all  $t \in (t_i, t_{i+1}), j \in \mathbb{N}$  with  $(\hat{u}^0, \hat{v}^0)^T \in L^2((0, 1); \mathbb{R}^2)$ , where

$$\tilde{u} := u - \hat{u},\tag{11}$$

$$\tilde{v} \coloneqq v - \hat{v},\tag{12}$$

are the observer errors satisfying

$$\tilde{u}_t(x,t) + \lambda_1 \tilde{u}_x(x,t) = c_1(x)\tilde{v}(x,t) - p_1(x)\tilde{u}(1,t), \tag{13}$$

$$\tilde{v}_t(x,t) - \lambda_2 \tilde{v}_x(x,t) = c_2(x)\tilde{u}(x,t) - p_2(x)\tilde{u}(1,t), \tag{14}$$

for all  $x \in (0, 1)$ , with boundary conditions

$$\tilde{u}(0,t) = q\tilde{v}(0,t),\tag{15}$$

$$\tilde{v}(1,t) = 0, \tag{16}$$

for all t>0. The terms  $p_1(x)$  and  $p_2(x)$  are the observer gains satisfying

$$p_1(x) = -\lambda_1 P^{\alpha\alpha}(x, 1), \tag{17}$$

$$p_2(x) = -\lambda_1 P^{\beta\alpha}(x, 1). \tag{18}$$

The gains  $p_1(x)$ ,  $p_2(x)$  are determined using the PDE backstepping technique equipped with the Volterra transformations

$$\tilde{u}(x,t) = \tilde{\alpha}(x,t) - \int_{x}^{1} P^{\alpha\alpha}(x,y)\tilde{\alpha}(y,t)dy$$

$$- \int_{x}^{1} P^{\alpha\beta}(x,y)\tilde{\beta}(y,t)dy,$$

$$\tilde{v}(x,t) = \tilde{\beta}(x,t) - \int_{x}^{1} P^{\beta\alpha}(x,y)\tilde{\alpha}(y,t)dy$$
(19)

$$-\int_{x}^{1} P^{\beta\beta}(x,y)\tilde{\beta}(y,t)dy, \qquad (20)$$

defined in the triangular domain  $0 \le x \le y \le 1$ . The readers are referred to Vazquez et al. (2011) for details on the kernels  $P^{\alpha\alpha}$ ,  $P^{\alpha\beta}$ ,  $P^{\beta\alpha}$ ,  $P^{\beta\beta}$ . Under the transformations (19), (20), and the observer gains (17), (18), the observer error system (13)–(16) gets transformed into the following observer error target system

$$\tilde{\alpha}_t(x,t) + \lambda_1 \tilde{\alpha}_x(x,t) = 0, \forall x \in (0,1), \tag{21}$$

$$\tilde{\beta}_t(x,t) - \lambda_2 \tilde{\beta}_x(x,t) = 0, \forall x \in (0,1), \tag{22}$$

$$\tilde{\alpha}(0,t) = q\tilde{\beta}(0,t),\tag{23}$$

$$\tilde{\beta}(1,t) = 0, \tag{24}$$

for all t > 0. The inverse transformations of (19), (20) take the form

$$\tilde{\alpha}(x,t) = \tilde{u}(x,t) + \int_{x}^{1} Q^{uu}(x,y)\tilde{u}(y,t)dy + \int_{x}^{1} Q^{uv}(x,y)\tilde{v}(y,t)dy,$$
(25)

$$\tilde{\beta}(x,t) = \tilde{v}(x,t) + \int_{x}^{1} Q^{vu}(x,y)\tilde{u}(y,t)dy + \int_{x}^{1} Q^{vv}(x,y)\tilde{v}(y,t)dy,$$
(26)

where the inverse kernels  $Q^{uv}$ ,  $Q^{vv}$ ,  $Q^{vv}$ ,  $Q^{vv}$  are defined in the domain  $0 \le x \le y \le 1$ . The readers are referred to Vazquez et al. (2011) for details on the kernels. The well-posedness of the closed-loop system (1)–(4), (7)–(10) with piecewise constant inputs between two sampling instants is established in the following proposition.

**Proposition 1** (*Espitia*, 2020). For any  $U_j \in \mathbb{R}$ ,  $(u(\cdot, t_j), v(\cdot, t_j))^T \in L^2((0, 1); \mathbb{R}^2)$ , and  $(\hat{u}(\cdot, t_j), \hat{v}(\cdot, t_j))^T \in L^2((0, 1); \mathbb{R}^2)$ , there exist unique solutions  $(u, v)^T \in C^0([t_j, t_{j+1}]; L^2((0, 1);$ 

 $\mathbb{R}^2$ )) and  $(\hat{u}, \hat{v})^T \in C^0([t_j, t_{j+1}]; L^2((0, 1); \mathbb{R}^2))$  to the systems (1)–(4) and (7)–(10), respectively, between two time instants  $t_i$  and  $t_{i+1}$ .

Let us consider the following sampled-data boundary control law

$$U(t_j) := U_j = \int_0^1 N^u(y)\hat{u}(y, t_j)dy + \int_0^1 N^v(y)\hat{v}(y, t_j)dy, \tag{27}$$

for all  $t \in [t_i, t_{i+1}), j \in \mathbb{N}$ , where  $N^u$  and  $N^v$  are the control gains

$$N^{u}(y) = K^{vu}(1, y) - \rho K^{uu}(1, y), \tag{28}$$

$$N^{v}(y) = K^{vv}(1, y) - \rho K^{uv}(1, y). \tag{29}$$

The readers are referred to Vazquez et al. (2011) for details on the gain kernels  $K^{uu}$ ,  $K^{uv}$ ,  $K^{vv}$ ,  $K^{vv}$  defined in the triangular domain  $0 \le y \le x \le 1$ . The control gains  $N^u$  and  $N^v$  are derived via the PDE backstepping technique equipped with the Volterra transformations

$$\hat{\alpha}(x,t) = \hat{u}(x,t) - \int_0^x K^{uu}(x,y)\hat{u}(y,t)dy - \int_0^x K^{uv}(x,y)\hat{v}(y,t)dy,$$
(30)

$$\hat{\beta}(x,t) = \hat{v}(x,t) - \int_{0}^{x} K^{vu}(x,y)\hat{u}(y,t)dy - \int_{0}^{x} K^{vv}(x,y)\hat{v}(y,t)dy,$$
(31)

defined in the domain  $0 \le y \le x \le 1$ . Subject to the transformations (30), (31), and the control input (27)–(29), the observer (7)–(10) gets transformed into the following observer target system

$$\hat{\alpha}_t(x,t) + \lambda_1 \hat{\alpha}_x(x,t) = \bar{p}_1(x)\tilde{\alpha}(1,t), \ \forall x \in (0,1),$$

$$\hat{\beta}_t(x,t) - \lambda_2 \hat{\beta}_x(x,t) = \bar{p}_2(x)\tilde{\alpha}(1,t), \ \forall x \in (0,1),$$
 (33)

$$\hat{\alpha}(0,t) = q\hat{\beta}(0,t),\tag{34}$$

$$\hat{\beta}(1,t) = \rho \tilde{\alpha}(1,t) + \rho \hat{\alpha}(1,t) + d(t), \tag{35}$$

for all  $t \in (t_j, t_{j+1}), j \in \mathbb{N}$ , where

$$\bar{p}_{1}(x) = p_{1}(x) - \int_{0}^{x} K^{uu}(x, y) p_{1}(y) dy - \int_{0}^{x} K^{uv}(x, y) p_{2}(y) dy,$$
(36)

$$\bar{p}_{2}(x) = p_{2}(x) - \int_{0}^{x} K^{vu}(x, y) p_{1}(y) dy - \int_{0}^{x} K^{vv}(x, y) p_{2}(y) dy,$$
(37)

for all  $x \in (0, 1)$ , and d(t) is the control input sampling error defined as

$$d(t) := U(t_j) - U(t) = \int_0^1 N^u(y) (\hat{u}(y, t_j) - \hat{u}(y, t)) dy + \int_0^1 N^v(y) (\hat{v}(y, t_j) - \hat{v}(y, t)) dy,$$
(38)

for all  $t \in (t_j, t_{j+1}), j \in \mathbb{N}$ .

The inverse transformations of (30), (31) take the form

$$\hat{u}(x,t) = \hat{\alpha}(x,t) + \int_0^x L^{\alpha\alpha}(x,y)\hat{\alpha}(y,t)dy + \int_0^x L^{\alpha\beta}(x,y)\hat{\beta}(y,t)dy,$$

$$\hat{v}(x,t) = \hat{\beta}(x,t) + \int_0^x L^{\beta\alpha}(x,y)\hat{\alpha}(y,t)dy$$
(39)

$$+ \int_0^x L^{\beta\beta}(x,y)\hat{\beta}(y,t)dy, \tag{40}$$

where the inverse kernels  $L^{\alpha\alpha}$ ,  $L^{\alpha\beta}$ ,  $L^{\beta\alpha}$ ,  $L^{\beta\beta}$  are defined in the domain  $0 \le y \le x \le 1$ . The readers are referred to Vazquez et al. (2011) for details on the inverse kernels.

The control input  $U_j$  given by (27) can also be expressed in terms of the inverse kernels and target system states  $(\hat{\alpha}, \hat{\beta})$  as Espitia (2020)

$$U(t_j) := U_j = \int_0^1 N^{\alpha}(y)\hat{\alpha}(y, t_j)dy + \int_0^1 N^{\beta}(y)\hat{\beta}(y, t_j)dy,$$
 (41)

for all  $t \in [t_j, t_{j+1}), j \in \mathbb{N}$ , where  $N^{\alpha}$  and  $N^{\beta}$  are given by

$$N^{\alpha}(\mathbf{y}) = L^{\beta\alpha}(1, \mathbf{y}) - \rho L^{\alpha\alpha}(1, \mathbf{y}), \tag{42}$$

$$N^{\beta}(y) = L^{\beta\beta}(1, y) - \rho L^{\alpha\beta}(1, y).$$
 (43)

Accordingly, the control input sampling error can be rewritten as

$$d(t) = \int_0^1 N^{\alpha}(y) (\hat{\alpha}(y, t_j) - \hat{\alpha}(y, t)) dy$$

$$+ \int_0^1 N^{\beta}(y) (\hat{\beta}(y, t_j) - \hat{\beta}(y, t)) dy,$$

$$(44)$$

for all  $t \in (t_j, t_{j+1}), j \in \mathbb{N}$ . We use  $U_j$  given by (41)–(43) and d(t) given by (44) in the event-triggering mechanisms to follow.

#### 3. Continuous-time event-triggered control (CETC)

In this section, we present an ETC design that prescribes control updates only at specific events but requires continuous evaluation of the triggering function to detect these events, hence the term continuous-time event-triggering. The triggering mechanism involves designing a switching dynamic variable that accounts for the effects of control input sampling, thereby preserving the GES of the closed-loop system. The details of the design are presented below.

**Definition 1.** Let  $\eta, \theta, \kappa_1, \kappa_2, \kappa_3, \kappa_4 > 0$  be event-trigger parameters. The set of event times  $I = \{t_j\}_{j \in \mathbb{N}}$  under CETC, which forms an increasing sequence satisfying  $\lim_{j \to \infty} t_j = +\infty$ , is defined by the following rule:

$$t_{j+1} = \inf \left\{ t \ge t_j + \tau | m(t) < 0 \right\}, \tag{45}$$

with  $t_0 = 0$ , where  $\tau > 0$  is the MDT to be specified, and m(t) evolves according to

$$\dot{m}(t) = -\eta m(t) + \kappa_1 \|\hat{\alpha}[t]\|^2 + \kappa_2 \|\hat{\beta}[t]\|^2 + \kappa_3 \hat{\alpha}^2(1, t) + \kappa_4 \tilde{\alpha}^2(1, t),$$
(46)

for all  $t \in (t_j, t_j + \tau)$ ,  $j \in \mathbb{N}$ , and

$$\dot{m}(t) = -\eta m(t) - \theta d^{2}(t) + \kappa_{1} \|\hat{\alpha}[t]\|^{2} + \kappa_{2} \|\hat{\beta}[t]\|^{2} + \kappa_{3} \hat{\alpha}^{2}(1, t) + \kappa_{\delta} \tilde{\alpha}^{2}(1, t).$$
(47)

for all  $t \in (t_j + \tau, t_{j+1})$ ,  $j \in \mathbb{N}$ , with  $m(t_0) = m(0) = 0$ ,  $m(t_j) \geq 0$ ,  $j \in \mathbb{N}_{>0}$  to be chosen appropriately at each event time, and  $m((t_j + \tau)^-) = m(t_j + \tau)$ ,  $j \in \mathbb{N}$ . In (46) and (47),  $\hat{\alpha}[t]$  and  $\hat{\beta}[t]$  are defined in (30) and (31), respectively. In (47), d(t) is given in (44). From (11) and (19), it follows that  $\tilde{\alpha}(1, t) = \tilde{u}(1, t) = u(1, t) - \hat{u}(1, t)$ .

**Assumption 2** (Event-trigger Parameter Selection). The parameters  $\eta, \kappa_1, \kappa_2, \kappa_3, \kappa_4 > 0$  are free parameters, and the parameter  $\theta > 0$  is chosen as

$$\theta = a_2 \omega_0^2 + a_1 \omega_0 + a_0, \tag{48}$$

where  $a_1, a_2, \omega_0 > 0$ , and

$$a_0 = 3Cq^2 e^{\frac{\mu}{\lambda_2}} + \frac{\varepsilon_0}{a_2}. (49)$$

Here

$$\varepsilon_0 = 5\lambda_2^2 \left( N^{\beta}(1) \right)^2, \tag{50}$$

where  $N^{\beta}(y)$  is given in (43), and subject to Assumption 1, the parameter  $\mu$  is selected such that

$$0 < \mu < \frac{\lambda_1 \lambda_2}{\lambda_1 + \lambda_2} \ln \left( \frac{1}{3\rho^2 q^2} \right), \tag{51}$$

and C > 0 is chosen to satisfy

$$C > \max \left\{ \frac{e^{\frac{\mu}{\lambda_1}}}{1 - 3\rho^2 q^2 e^{\mu\left(\frac{1}{\lambda_1} + \frac{1}{\lambda_2}\right)}} \left(\frac{\varepsilon_3}{a_2} + \kappa_3\right), \frac{1}{\mu - \delta} \left(\frac{\max\{\varepsilon_1, \varepsilon_2\}r}{a_2} + \max\{\kappa_1, \kappa_2\}r\right) \right\},$$
 (52)

for some  $\delta > 0$  such that  $\delta < \mu$ , and

$$r = \frac{1}{\min\left\{\frac{1}{\lambda_1}e^{-\frac{\mu}{\lambda_1}}, \frac{q^2}{\lambda_2}\right\}},\tag{53}$$

$$\varepsilon_1 = 5\lambda_1^2 \int_0^1 \left( \dot{N}^{\alpha}(y) \right)^2 dy, \tag{54}$$

$$\varepsilon_2 = 5\lambda_2^2 \int_0^1 \left( \dot{N}^\beta(y) \right)^2 dy, \tag{55}$$

$$\varepsilon_3 = 5 \left( \lambda_1 N^{\alpha}(1) - \rho \lambda_2 N^{\beta}(1) \right)^2. \tag{56}$$

Here,  $N^{\alpha}(y)$  is given in (42).

**Theorem 1.** Consider a set of increasing event times  $I = \{t_j\}_{j \in \mathbb{N}}$  with  $t_0 = 0$ , satisfying  $\lim_{j \to \infty} t_j = +\infty$ , generated by the CETC triggering rule in Definition 1. For every  $(u(\cdot,0),v(\cdot,0))^T \in L^2((0,1);\mathbb{R}^2)$ , and  $(\hat{u}(\cdot,0),\hat{v}(\cdot,0))^T \in L^2((0,1);\mathbb{R}^2)$ , there exist unique solutions  $(u,v)^T \in C^0(\mathbb{R}_{>0};L^2((0,1);\mathbb{R}^2))$  and  $(\hat{u},\hat{v})^T \in C^0(\mathbb{R}_{>0};L^2((0,1);\mathbb{R}^2))$  to (1)-(4), (7)-(10), (17), (18), (41)-(43). Choose the event-trigger parameters  $\eta,\theta,\kappa_1,\kappa_2,\kappa_3,\kappa_4>0$  as in Assumption 2, and the MDT  $\tau>0$  as

$$\tau = \int_{\omega_0}^{\omega_1} \frac{1}{a_2 s^2 + a_1 s + a_0} ds,\tag{57}$$

for any  $\omega_1 > \omega_0 > 0$ ,  $a_1$ ,  $a_2 > 0$ , and  $a_0 > 0$  given by (49). Further, choose the initial conditions of m(t) satisfying (46), (47) as

$$m(t_0) = m(0) = 0,$$
 (58)

$$m((t_i + \tau)^-) = m(t_i + \tau), \text{ for } j \in \mathbb{N}, \tag{59}$$

$$m(t_j) = \omega_0 d^2(t_i^-) = \omega_0 (U_{j-1} - U_j)^2, \text{ for } j \in \mathbb{N}_{>0},$$
 (60)

where  $U_j$ ,  $j \in \mathbb{N}$  given by (41) is the control input updated at  $t = t_j$ . Then, under the CETC triggering rule in Definition 1, the closed-loop system (1)–(4), (7)–(10), (17), (18), (41)–(43) is globally exponentially stable. More specifically, the following estimate holds:

$$\Phi(t) \le M_{\text{etc}} e^{-\frac{\nu_{\text{etc}}^*}{2}t} \Phi(0), \tag{61}$$

for all t > 0, where

$$\Phi(t) = \|u[t]\| + \|\hat{u}[t]\| + \|v[t]\| + \|\hat{v}[t]\|, \tag{62}$$

for some constants  $M_{\rm etc}$ ,  $v_{\rm etc}^{\star} > 0$ .

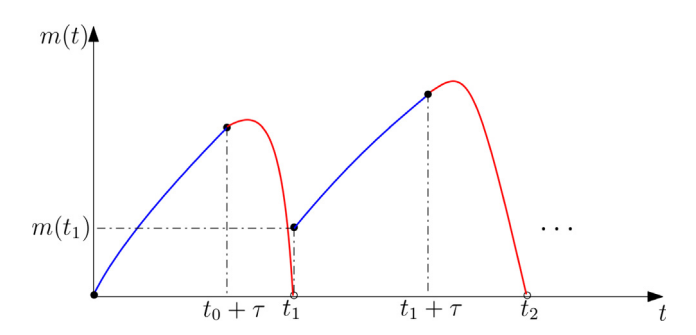


**Fig. 1.** A schematic of evolution of m(t). Note that  $m(t_0)=0$  and  $m((t_j+\tau)^-)=m(t_j+\tau), j\in\mathbb{N}$ , whereas  $m(t_j)\geq 0, j\in\mathbb{N}_{>0}$  is appropriately chosen at each event  $t=t_j$ .

**Remark 2.** Using partial fraction expansion, it can be shown that the MDT  $\tau > 0$  chosen as (57) can be expressed as

$$\tau = \begin{cases} \frac{\omega_{1} - \omega_{0}}{a_{2} \left(\omega_{1} + \frac{a_{1}}{2a_{2}}\right) \left(\omega_{0} + \frac{a_{1}}{2a_{2}}\right)}, & \text{if } \Delta = 0, \\ \frac{1}{\sqrt{\Delta}} \ln \left(1 + \frac{\frac{\sqrt{\Delta}}{a_{2}} (\omega_{1} - \omega_{0})}{\left(\omega_{1} + \frac{a_{1} + \sqrt{\Delta}}{2a_{2}}\right) \left(\omega_{0} + \frac{a_{1} - \sqrt{\Delta}}{2a_{2}}\right)}\right), & \text{if } \Delta > 0, \\ \frac{2}{\sqrt{-\Delta}} \left(\tan^{-1} \left(\frac{\frac{2a_{2}}{\sqrt{-\Delta}} (\omega_{1} - \omega_{0})}{1 - \frac{4a_{2}^{2}}{\Delta} \left(\omega_{1} + \frac{a_{1}}{2a_{2}}\right) \left(\omega_{0} + \frac{a_{1}}{2a_{2}}\right)}\right)\right), & \text{if } \Delta < 0, \end{cases}$$
(63)

where

$$\Delta := a_1^2 - 4a_0a_2. \tag{64}$$

In the following subsection, we complete the proof of Theorem 1.

# 3.1. Proof of Theorem 1

# 3.1.1. Preliminaries

Before proceeding to the proof of Theorem 1, we provide several necessary auxiliary results below in Lemmas 1–3.

**Lemma 1.** Consider a set of increasing event times  $I = \{t_j\}_{j \in \mathbb{N}}$  with  $t_0 = 0$ , satisfying  $\lim_{j \to \infty} t_j = +\infty$ , generated by the CETC triggering rule in Definition 1. Then, for the dynamic variable m(t) governed by (46), (47) with m(0) = 0,  $m(t_j) \ge 0$ ,  $j \in \mathbb{N}_{>0}$  to be chosen, and  $m((t_j + \tau)^-) = m(t_j + \tau)$ ,  $j \in \mathbb{N}$  for any  $\tau > 0$ , it holds that  $m(t) \ge 0$  for all t > 0.

**Proof.** Let  $m(t_0) = 0$  and  $m(t_j), j \in \mathbb{N}_{>0}$  be such that  $m(t_j) \geq 0$ . Then, we have from (46) that

$$m(t) = e^{-\eta(t-t_j)} m(t_j) + \int_{t_j}^t e^{-\eta(t-\xi)} \left( \kappa_1 \|\hat{\alpha}[\xi]\|^2 + \kappa_2 \|\hat{\beta}[\xi]\|^2 + \kappa_3 \hat{\alpha}^2(1,\xi) + \kappa_4 \tilde{\alpha}^2(1,\xi) \right) d\xi \ge 0,$$
(65)

for all  $t \in (t_j, t_j + \tau], j \in \mathbb{N}$ . After  $t = t_j + \tau$ , the variable m(t) evolves according to (47), and an event would trigger at  $t = t_{j+1}$  according to (45) to ensure that  $m(t) \geq 0$  for all  $t \in (t_j + \tau, t_{j+1}), j \in \mathbb{N}$ . Following the same line of reasoning, starting with  $m(t_0) = 0$ , it can be shown that  $m(t) \geq 0$  for all t > 0.

In Fig. 1, we have shown a schematic of evolution of m(t).

**Lemma 2.** Consider a set of increasing event times  $I = \{t_j\}_{j \in \mathbb{N}}$  with  $t_0 = 0$ , satisfying  $\lim_{j \to \infty} t_j = +\infty$ , generated by the CETC

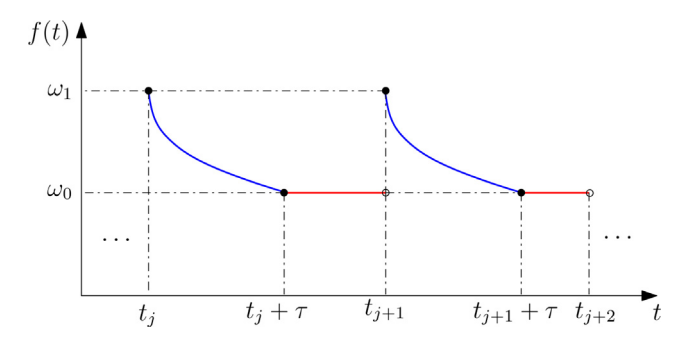


**Fig. 2.** A schematic of evolution of the reset function f(t). Note that  $f(t_j) = \omega_1$ ,  $f((t_j + \tau)^-) = f(t_j + \tau) = \omega_0$ , and  $f(t) = \omega_0$  for all  $t \in [t_j + \tau, t_{j+1}), j \in \mathbb{N}$ .

triggering rule in Definition 1. Then, for d(t) given by (44), it holds that

$$(\dot{d}(t))^2 \le \varepsilon_0 d^2(t) + \varepsilon_1 \|\hat{\alpha}[t]\|^2 + \varepsilon_2 \|\hat{\beta}[t]\|^2$$

$$+ \varepsilon_3 \hat{\alpha}^2(1, t) + \varepsilon_4 \tilde{\alpha}^2(1, t), \tag{66}$$

for all  $t \in (t_j, t_{j+1}), j \in \mathbb{N}$ , where  $\varepsilon_0, \varepsilon_1, \varepsilon_2, \varepsilon_3 > 0$  are given by (50), (54)–(56), respectively, and

$$\varepsilon_4 = 5 \left( \int_0^1 \left( N^{\alpha}(y) \bar{p}_1(y) + N^{\beta}(y) \bar{p}_2(y) \right) dy + \rho \lambda_2 N^{\beta}(1) \right)^2. \tag{67}$$

Here,  $N^{\alpha}(y)$ ,  $\bar{p}_1(y)$ , and  $\bar{p}_2(y)$  are given in (42), (17), and (18), respectively.

The proof is very similar to that of Lemma 2 in Espitia (2020), and hence is omitted.

**Lemma 3.** Consider a set of increasing event times  $I = \{t_j\}_{j \in \mathbb{N}}$  with  $t_0 = 0$ , satisfying  $\lim_{j \to \infty} t_j = +\infty$ , generated by the CETC triggering rule in Definition 1. Let the MDT  $\tau > 0$  be chosen as in (57), for any  $a_0$ ,  $a_1$ ,  $a_2 > 0$  and  $\omega_1 > \omega_0 > 0$ . Then, for a piecewise right-continuous reset function  $f(t) : \mathbb{R}_{>0} \to \mathbb{R}_{>0}$  satisfying

$$\dot{f}(t) = \begin{cases} -a_2 f^2(t) - a_1 f(t) - a_0, & \text{for all } t \in (t_j, t_j + \tau), \\ 0, & \text{for all } t \in (t_j + \tau, t_{j+1}), \end{cases}$$
(68)

for all  $j \in \mathbb{N}$ , with  $f(t_j) = \omega_1 > 0$  and  $f((t_j + \tau)^-) = f(t_j + \tau)$ , it follows that f(t) strictly decreases from  $f(t_j) = \omega_1$  to  $f(t_j + \tau) = \omega_0$  over  $t \in [t_j, t_j + \tau)$ , and remains constant at  $f(t) = \omega_0$  for all  $t \in [t_j + \tau, t_{j+1})$ .

**Proof.** Considering (68) and noting that  $\tau>0$  is chosen as in (57), we can straightforwardly show that f(t) goes from  $\omega_1>0$  to  $\omega_0>0$  when t goes from  $t=t_j$  to  $t=t_j+\tau$ . We can also observe from (68) for all  $t\in (t_j,t_j+\tau)$  that  $\dot{f}(t)$  is negative when  $f(t)\geq 0$ , forcing f(t) to strictly decrease. Thus, the function f(t) strictly decreases for all  $t\in [t_j,t_j+\tau)$  from  $f(t_j)=\omega_1$  to  $f(t_j+\tau)=\omega_0$ . However, since  $\dot{f}(t)=0$  for all  $t\in (t_j+\tau,t_{j+1})$ , the function f(t) remains constant at  $f(t)=\omega_0$  for all  $t\in [t_j+\tau,t_{j+1})$ .

In Fig. 2, we have shown a schematic of evolution of the reset function f(t).

#### 3.1.2. Main proof

With Proposition 1 and Lemmas 1–3 in hand, we are now in a position to proceed with the proof of Theorem 1.

The well-posedness, in the sense of Theorem 1, is established by applying Proposition 1 iteratively between events. It follows from Lemma 1 that  $m(t) \ge 0$  for all t > 0, and from Lemma 3 that f(t) > 0 for all t > 0 if the MDT  $\tau > 0$  is chosen as (57). Thus, we consider the following Lyapunov candidate:

$$W_2(t) = W_1(t) + f(t)d^2(t) + m(t), (69)$$

where

$$W_1(t) = V_1(t) + V_2(t), (70)$$

with

$$V_1(t) = \int_0^1 \left( \frac{A}{\lambda_1} \tilde{\alpha}^2(x, t) e^{-\frac{\mu x}{\lambda_1}} + \frac{B}{\lambda_2} \tilde{\beta}^2(x, t) e^{\frac{\mu x}{\lambda_2}} \right) dx, \tag{71}$$

$$V_2(t) = \int_0^1 \left( \frac{C}{\lambda_1} \hat{\alpha}^2(x, t) e^{-\frac{\mu x}{\lambda_1}} + \frac{D}{\lambda_2} \hat{\beta}^2(x, t) e^{\frac{\mu x}{\lambda_2}} \right) dx. \tag{72}$$

Let the parameter  $\mu > 0$  be chosen as in (51), C > 0 be chosen as in (52), A > 0 be chosen such that

$$A > e^{\frac{\mu}{\lambda_{1}}} \left( \frac{C \|\bar{p}_{1}\|^{2}}{\lambda_{1}\delta} + \frac{Cq^{2} \|\bar{p}_{2}\|^{2} e^{\frac{\mu}{\lambda_{2}}}}{\lambda_{2}\delta} + 3C\rho^{2}q^{2}e^{\frac{\mu}{\lambda_{2}}} + \frac{\varepsilon_{4}}{a_{2}} + \kappa_{4} \right), \tag{73}$$

for some  $\delta>0$  such that  $\mu>\delta$ , and B,D>0 to be chosen later. In (71) and (72),  $(\tilde{\alpha},\tilde{\beta})$  satisfies (21)–(24) for all t>0, and  $(\hat{\alpha},\hat{\beta})$  satisfies (32)–(35) for all  $t\in(t_j,t_{j+1}), j\in\mathbb{N}$ . Taking the time derivative of  $V_1(t)$  and  $V_2(t)$  for all  $t\in(t_j,t_{j+1}), j\in\mathbb{N}$  and integrating by parts, we obtain that

$$\dot{V}_1(t) = -\mu V_1(t) - A\tilde{\alpha}^2(1, t)e^{-\frac{\mu}{\lambda_1}} - (B - Aq^2)\tilde{\beta}^2(0, t), \tag{74}$$

and

$$\dot{V}_{2}(t) = -\mu V_{2}(t) + \frac{2C}{\lambda_{1}} \left( \int_{0}^{1} \hat{\alpha}(x, t) \bar{p}_{1}(x) e^{-\frac{\mu x}{\lambda_{1}}} dx \right) \tilde{\alpha}(1, t) 
+ \frac{2D}{\lambda_{2}} \left( \int_{0}^{1} \hat{\beta}(x, t) \bar{p}_{2}(x) e^{\frac{\mu x}{\lambda_{2}}} dx \right) \tilde{\alpha}(1, t)$$
(75)

 $-C\hat{\alpha}^2(1,t)e^{-\frac{\mu}{\lambda_1}}-(D-Cq^2)\hat{\beta}^2(0,t)+D\hat{\beta}^2(1,t)e^{\frac{\mu}{\lambda_2}}$ . From Young's and Cauchy–Schwarz inequalities and considering (35), we obtain that

$$\hat{\beta}^{2}(1,t) \leq 3d^{2}(t) + 3\rho^{2}\tilde{\alpha}^{2}(1,t) + 3\rho^{2}\hat{\alpha}^{2}(1,t), \tag{76}$$

$$2\left(\int_{0}^{1}\hat{\alpha}(x,t)\bar{p}_{1}(x)e^{-\frac{\mu x}{\lambda_{1}}}dx\right)\tilde{\alpha}(1,t) \leq \delta\int_{0}^{1}\hat{\alpha}^{2}(x,t)e^{-\frac{\mu x}{\lambda_{1}}}dx$$

$$+ \frac{\|\bar{p}_1\|^2}{s} \tilde{\alpha}^2(1, t), \tag{77}$$

$$2\left(\int_{0}^{1} \hat{\beta}(x,t)\bar{p}_{2}(x)e^{\frac{\mu x}{\lambda_{2}}}dx\right)\tilde{\alpha}(1,t) \leq \delta \int_{0}^{1} \hat{\beta}^{2}(x,t)e^{\frac{\mu x}{\lambda_{2}}}dx + \frac{\|\bar{p}_{2}\|^{2}e^{\frac{\mu}{\lambda_{2}}}}{\delta}\tilde{\alpha}^{2}(1,t),$$
(78)

for all  $t \ge 0$ , for some  $\delta > 0$ . Thus, we write from (74), (75) that

$$\begin{split} \dot{V}_{1}(t) + \dot{V}_{2}(t) &\leq -\mu V_{1}(t) - \mu V_{2}(t) + \delta V_{2}(t) \\ - \left( Ce^{-\frac{\mu}{\lambda_{1}}} - 3\rho^{2}De^{\frac{\mu}{\lambda_{2}}} \right) \hat{\alpha}^{2}(1,t) - (D - Cq^{2})\hat{\beta}^{2}(0,t) \\ - \left( Ae^{-\frac{\mu}{\lambda_{1}}} - \frac{C\|\bar{p}_{1}\|^{2}}{\lambda_{1}\delta} - \frac{D\|\bar{p}_{2}\|^{2}e^{\frac{\mu}{\lambda_{2}}}}{\lambda_{2}\delta} - 3\rho^{2}De^{\frac{\mu}{\lambda_{2}}} \right) \tilde{\alpha}^{2}(1,t) \\ - (B - Aq^{2})\tilde{\beta}^{2}(0,t) + 3De^{\frac{\mu}{\lambda_{2}}}d^{2}(t), \end{split}$$
(79)

for all  $t \in (t_j, t_{j+1}), j \in \mathbb{N}$ . Let us choose  $B = Aq^2$  and  $D = Cq^2$ . Then, (79) reduces to

$$\dot{V}_{1}(t) + \dot{V}_{2}(t) \leq -\mu V_{1}(t) - \mu V_{2}(t) + \delta V_{2}(t) 
- Ce^{-\frac{\mu}{\lambda_{1}}} \left( 1 - 3\rho^{2}q^{2}e^{\mu\left(\frac{1}{\lambda_{1}} + \frac{1}{\lambda_{2}}\right)} \right) \hat{\alpha}^{2}(1, t) 
- \left( Ae^{-\frac{\mu}{\lambda_{1}}} - \frac{C\|\bar{p}_{1}\|^{2}}{\lambda_{1}\delta} - \frac{Cq^{2}\|\bar{p}_{2}\|^{2}e^{\frac{\mu}{\lambda_{2}}}}{\lambda_{2}\delta} 
- 3C\rho^{2}q^{2}e^{\frac{\mu}{\lambda_{2}}} \right) \tilde{\alpha}^{2}(1, t) + 3Cq^{2}e^{\frac{\mu}{\lambda_{2}}}d^{2}(t),$$
(80)

valid for all  $t \in (t_j, t_{j+1}), j \in \mathbb{N}$ . Now let us consider  $W_2(t)$  given by (69) for all  $t \in (t_j, t_j + \tau), j \in \mathbb{N}$ .

For all  $t \in (t_i, t_i + \tau), j \in \mathbb{N}$ :

Taking the time derivative of (69) for all  $t \in (t_j, t_j + \tau)$ ,  $j \in \mathbb{N}$ , using Young's inequality, and considering (46), (66), (68), (80), we write that

$$\begin{split} \dot{W}_{2}(t) &= \dot{V}_{1}(t) + \dot{V}_{2}(t) + \dot{f}(t)d^{2}(t) + 2f(t)d(t)\dot{d}(t) + \dot{m}(t) \\ &\leq \dot{V}_{1}(t) + \dot{V}_{2}(t) + \dot{f}(t)d^{2}(t) + a_{2}f^{2}(t)d^{2}(t) \\ &+ \frac{1}{a_{2}} \left( \dot{d}(t) \right)^{2} + \dot{m}(t) \\ &\leq -\mu V_{1}(t) - \mu V_{2}(t) + \delta V_{2}(t) \\ &- Ce^{-\frac{\mu}{\lambda_{1}}} \left( 1 - 3\rho^{2}q^{2}e^{\mu\left(\frac{1}{\lambda_{1}} + \frac{1}{\lambda_{2}}\right)} \right) \hat{\alpha}^{2}(1, t) \\ &- \left( Ae^{-\frac{\mu}{\lambda_{1}}} - \frac{C \|\bar{p}_{1}\|^{2}}{\lambda_{1}\delta} - \frac{Cq^{2}\|\bar{p}_{2}\|^{2}e^{\frac{\mu}{\lambda_{2}}}}{\lambda_{2}\delta} \right) \\ &- 3C\rho^{2}q^{2}e^{\frac{\mu}{\lambda_{2}}} \hat{\alpha}^{2}(1, t) \\ &+ 3Cq^{2}e^{\frac{\mu}{\lambda_{2}}}d^{2}(t) - \left( a_{2}f^{2}(t) + a_{1}f(t) + a_{0} \right)d^{2}(t) \\ &+ a_{2}f^{2}(t)d^{2}(t) + \frac{\varepsilon_{0}}{a_{2}}d^{2}(t) + \frac{\varepsilon_{1}}{a_{2}} \|\hat{\alpha}[t]\|^{2} + \frac{\varepsilon_{2}}{a_{2}} \|\hat{\beta}[t]\|^{2} \\ &+ \frac{\varepsilon_{3}}{a_{2}}\hat{\alpha}^{2}(1, t) + \frac{\varepsilon_{4}}{a_{2}}\tilde{\alpha}^{2}(1, t) - \eta m(t) + \kappa_{1} \|\hat{\alpha}[t]\|^{2} \\ &+ \kappa_{2} \|\hat{\beta}[t]\|^{2} + \kappa_{3}\hat{\alpha}^{2}(1, t) + \kappa_{4}\tilde{\alpha}^{2}(1, t), \end{split}$$

for some  $a_2>0$ . Note from (72) that we can write recalling our choice  $D=Cq^2$  that

$$\|\hat{\alpha}[t]\|^2 + \|\hat{\beta}[t]\|^2 \le \frac{r}{C}V_2(t),$$
 (82)

for all  $t \ge 0$ , where r is given by (53). Therefore, (81) can be rewritten as

$$\begin{split} \dot{W}_{2}(t) &\leq -\mu V_{1}(t) \\ &- \left( \mu - \delta - \frac{\max\{\varepsilon_{1}, \varepsilon_{2}\}r}{Ca_{2}} - \frac{\max\{\kappa_{1}, \kappa_{2}\}r}{C} \right) V_{2}(t) \\ &- \left( Ce^{-\frac{\mu}{\lambda_{1}}} \left( 1 - 3\rho^{2}q^{2}e^{\mu\left(\frac{1}{\lambda_{1}} + \frac{1}{\lambda_{2}}\right)} \right) - \frac{\varepsilon_{3}}{a_{2}} - \kappa_{3} \right) \hat{\alpha}^{2}(1, t) \\ &- \left( Ae^{-\frac{\mu}{\lambda_{1}}} - \frac{C\|\bar{p}_{1}\|^{2}}{\lambda_{1}\delta} - \frac{Cq^{2}\|\bar{p}_{2}\|^{2}e^{\frac{\mu}{\lambda_{2}}}}{\lambda_{2}\delta} \right. \\ &- 3C\rho^{2}q^{2}e^{\frac{\mu}{\lambda_{2}}} - \frac{\varepsilon_{4}}{a_{2}} - \kappa_{4} \right) \tilde{\alpha}^{2}(1, t) \\ &- a_{1}f(t)d^{2}(t) - \left( a_{0} - 3Cq^{2}e^{\frac{\mu}{\lambda_{2}}} - \frac{\varepsilon_{0}}{a_{2}} \right) d^{2}(t) - \eta m(t). \end{split}$$
 (83)

Let

$$v_{\text{etc}} := \mu - \delta - \frac{\max\{\varepsilon_1, \varepsilon_2\}r}{Ca_2} - \frac{\max\{\kappa_1, \kappa_2\}r}{C},\tag{84}$$

and note from (52) that choice of  $\delta>0$  such that  $\delta<\mu$  and the choice of C>0 ensures  $v_{\rm etc}>0$ . Furthermore, the same choice of C>0 in (52) ensures  $Ce^{-\frac{\mu}{\lambda_1}}\left(1-3\rho^2q^2e^{\mu\left(\frac{1}{\lambda_1}+\frac{1}{\lambda_2}\right)}\right)-\frac{\varepsilon_3}{a_2}-\kappa_3>0$  since the choice of  $\mu>0$  as in (51) subject to Assumption 1 leads to  $1-3\rho^2q^2e^{\mu\left(\frac{1}{\lambda_1}+\frac{1}{\lambda_2}\right)}>0$ . Therefore, noting that A>0 chosen as in (73) ensures  $Ae^{-\frac{\mu}{\lambda_1}}-\frac{C\|\bar{p}_1\|^2}{\lambda_1\delta}-\frac{Cq^2\|\bar{p}_2\|^2e^{\frac{\mu}{\lambda_2}}}{\lambda_2\delta}-3C\rho^2q^2e^{\frac{\mu}{\lambda_2}}-\frac{\varepsilon_4}{a_2}-\kappa_4>0$  and choosing  $a_0>0$  as (49), we rewrite (83) as

$$\dot{W}_{2}(t) \leq -\nu_{\text{etc}}W_{1}(t) - a_{1}f(t)d^{2}(t) - \eta m(t) 
\leq -\nu_{\text{etc}}^{\star}W_{2}(t),$$
(85)

for all  $t \in (t_j, t_j + \tau), j \in \mathbb{N}$ , where

$$\upsilon_{\text{etc}}^{\star} := \min\{\upsilon_{\text{etc}}, a_1, \eta\}. \tag{86}$$

For all  $t \in (t_i + \tau, t_{i+1}), j \in \mathbb{N}$ :

For all  $t \in (t_j + \tau, t_{j+1}), j \in \mathbb{N}$ , we have that  $f(t) = \omega_0 > 0$  (see Lemma 3). Taking the time derivative of (69) for all  $t \in (t_j + \tau, t_{j+1}), j \in \mathbb{N}$ , using Young's inequality, and considering (47), (66), (68), (80), we can write that

$$\dot{W}_{2}(t) = \dot{V}_{1}(t) + \dot{V}_{2}(t) + 2\omega_{0}d(t)\dot{d}(t) + \dot{m}(t) 
\leq \dot{V}_{1}(t) + \dot{V}_{2}(t) + a_{2}\omega_{0}^{2}d^{2}(t) + \frac{1}{a_{2}}(\dot{d}(t))^{2} + \dot{m}(t) 
\leq -\mu V_{1}(t) - \mu V_{2}(t) + \delta V_{2}(t) 
- Ce^{-\frac{\mu}{\lambda_{1}}} \left(1 - 3\rho^{2}q^{2}e^{\mu\left(\frac{1}{\lambda_{1}} + \frac{1}{\lambda_{2}}\right)}\right) \hat{\alpha}^{2}(1, t) 
- \left(Ae^{-\frac{\mu}{\lambda_{1}}} - \frac{C\|\bar{p}_{1}\|^{2}}{\lambda_{1}\delta} - \frac{Cq^{2}\|\bar{p}_{2}\|^{2}e^{\frac{\mu}{\lambda_{2}}}}{\lambda_{2}\delta} - 3C\rho^{2}q^{2}e^{\frac{\mu}{\lambda_{2}}}\right) \tilde{\alpha}^{2}(1, t) + 3Cq^{2}e^{\frac{\mu}{\lambda_{2}}}d^{2}(t) + a_{2}\omega_{0}^{2}d^{2}(t) 
+ \frac{\varepsilon_{0}}{a_{2}}d^{2}(t) + \frac{\varepsilon_{1}}{a_{2}}\|\hat{\alpha}[t]\|^{2} + \frac{\varepsilon_{2}}{a_{2}}\|\hat{\beta}[t]\|^{2} + \frac{\varepsilon_{3}}{a_{2}}\hat{\alpha}^{2}(1, t) 
+ \frac{\varepsilon_{4}}{a_{2}}\tilde{\alpha}^{2}(1, t) - \eta m(t) - \theta d^{2}(t) + \kappa_{1}\|\hat{\alpha}[t]\|^{2} 
+ \kappa_{2}\|\hat{\beta}[t]\|^{2} + \kappa_{3}\hat{\alpha}^{2}(1, t) + \kappa_{4}\tilde{\alpha}^{2}(1, t).$$
(87)

Recalling (82) and rearranging (87), we obtain that

$$\begin{split} \dot{W}_{2}(t) &\leq -\mu V_{1}(t) - \left(\mu - \delta - \frac{\max\{\varepsilon_{1}, \varepsilon_{2}\}r}{Ca_{2}}\right) \\ &- \frac{\max\{\kappa_{1}, \kappa_{2}\}r}{C}\right) V_{2}(t) \\ &- \left(Ce^{-\frac{\mu}{\lambda_{1}}} \left(1 - 3\rho^{2}q^{2}e^{\mu\left(\frac{1}{\lambda_{1}} + \frac{1}{\lambda_{2}}\right)}\right) \\ &- \frac{\varepsilon_{3}}{a_{2}} - \kappa_{3}\right) \hat{\alpha}^{2}(1, t) \\ &- \left(Ae^{-\frac{\mu}{\lambda_{1}}} - \frac{C\|\bar{p}_{1}\|^{2}}{\lambda_{1}\delta} - \frac{Cq^{2}\|\bar{p}_{2}\|^{2}e^{\frac{\mu}{\lambda_{2}}}}{\lambda_{2}\delta} \\ &- 3C\rho^{2}q^{2}e^{\frac{\mu}{\lambda_{2}}} - \frac{\varepsilon_{4}}{a_{2}} - \kappa_{4}\right) \tilde{\alpha}^{2}(1, t) \\ &- \left(\theta - 3Cq^{2}e^{\frac{\mu}{\lambda_{2}}} - \frac{\varepsilon_{0}}{a_{2}} - a_{2}\omega_{0}^{2}\right) d^{2}(t) - \eta m(t). \end{split}$$
(88)

By selecting  $\theta > 0$  as (48), (49), we simplify (88) to obtain

$$\dot{W}_{2}(t) \leq -\mu V_{1}(t) - \left(\mu - \delta - \frac{\max\{\varepsilon_{1}, \varepsilon_{2}\}r}{Ca_{2}}\right) \\
- \frac{\max\{\kappa_{1}, \kappa_{2}\}r}{C} V_{2}(t) \\
- \left(Ce^{-\frac{\mu}{\lambda_{1}}} \left(1 - 3\rho^{2}q^{2}e^{\mu\left(\frac{1}{\lambda_{1}} + \frac{1}{\lambda_{2}}\right)}\right) \\
- \frac{\varepsilon_{3}}{a_{2}} - \kappa_{3}\right) \hat{\alpha}^{2}(1, t) \\
- \left(Ae^{-\frac{\mu}{\lambda_{1}}} - \frac{C\|\bar{p}_{1}\|^{2}}{\lambda_{1}\delta} - \frac{Cq^{2}\|\bar{p}_{2}\|^{2}e^{\frac{\mu}{\lambda_{2}}}}{\lambda_{2}\delta} \\
- 3C\rho^{2}q^{2}e^{\frac{\mu}{\lambda_{2}}} - \frac{\varepsilon_{4}}{a_{2}} - \kappa_{4}\right) \tilde{\alpha}^{2}(1, t) \\
- a_{1}\omega_{0}d^{2}(t) - \eta m(t). \tag{89}$$

Then, following steps similar to (84)–(86) and recalling from Lemma 3 that  $f(t)=\omega_0>0$  for all  $t\in[t_j+\tau,t_{j+1}),j\in\mathbb{N}$ , we can show that

$$\dot{W}_2(t) \le -\upsilon_{\text{etc}}^{\star} W_2(t), \tag{90}$$

for all  $t \in (t_i + \tau, t_{i+1}), j \in \mathbb{N}$ .

Recall that  $m(t_j+\tau)$  is chosen such that  $m\big((t_j+\tau)^-\big)=m(t_j+\tau)$ , and from Lemma 3 that  $f\big((t_j+\tau)^-\big)=f(t_j+\tau)=\omega_0$ . Further, note that  $d\big((t_j+\tau)^-\big)=d(t_j+\tau)$  and that  $\|\hat{\alpha}[t]\|,\|\hat{\beta}[t]\|,\|\tilde{\alpha}[t]\|,\|\tilde{\beta}[t]\|$  are continuous. Thus, considering (85), (90), (69)–(72), it can be shown that

$$W_2(t) \le e^{-\upsilon_{\text{etc}}^{\star}(t-t_j)} W_2(t_i), \tag{91}$$

for all  $t \in (t_i, t_{i+1}), j \in \mathbb{N}$ . But we have that

$$W_{2}(t_{j}^{-}) = W_{1}(t_{j}^{-}) + f(t_{j}^{-})d^{2}(t_{j}^{-}) + m(t_{j}^{-})$$

$$= W_{1}(t_{j}^{-}) + \omega_{0}d^{2}(t_{j}^{-})$$

$$= W_{1}(t_{j}) + \omega_{0}d^{2}(t_{i}^{-}),$$
(92)

as  $f(t_j^-) = \omega_0$  (see Lemma 3) and  $m(t_j^-) = 0$  (since events are triggered according to (45)). On the other hand, we have that

$$W_2(t_i) = W_1(t_i) + f(t_i)d^2(t_i) + m(t_i) = W_1(t_i) + m(t_i),$$
(93)

as  $d(t_i) = 0$ . Thus, if  $m(t_i)$  is chosen as in (60), we have that

$$W_2(t_i^-) = W_2(t_j), \text{ for } j \in \mathbb{N}_{>0}.$$
 (94)

Therefore, using (91) and (94) recursively, we can show that

$$W_{2}(t) \leq e^{-\upsilon_{\text{etc}}^{\star}(t-t_{j})} W_{2}(t_{j}) = e^{-\upsilon_{\text{etc}}^{\star}(t-t_{j})} W_{2}(t_{j}^{-})$$

$$\leq e^{-\upsilon_{\text{etc}}^{\star}(t-t_{j})} \times e^{-\upsilon_{\text{etc}}^{\star}(t_{j}-t_{j-1})} W_{2}(t_{j-1})$$

$$\vdots$$

$$\leq e^{-\upsilon_{\text{etc}}^{\star}(t-t_{j})} \times \prod_{i=j}^{i=j} e^{-\upsilon_{\text{etc}}^{\star}(t_{i}-t_{i-1})} W_{2}(0)$$

$$= e^{-\upsilon_{\text{etc}}^{\star}t} W_{2}(0).$$
(95)

for all t > 0. But we have that

$$W_2(0) = W_1(0) + f(0)d^2(0) + m(0) = W_1(0), (96)$$

as d(0) = 0 and m(0) = 0, and

$$W_1(t) \le W_2(t), \tag{97}$$

for all  $t \ge 0$ . Thus, it follows from (95) that

$$W_1(t) \le e^{-v_{\text{etc}}^{\star}t} W_1(0),$$
 (98)

for all t > 0. Then, using the standard arguments of PDE back-stepping involving the bounded invertibility of the transformations (19), (20), (25), (26), (30), (31), (39), (40), we obtain (61). This completes the proof of Theorem 1.

Remark 3. In existing dynamic CETC approaches using PDE back-stepping for both parabolic PDEs (Demir, Koga, & Krstic, 2024; Rathnayake & Diagne, 2024a; Rathnayake et al., 2025; Rathnayake, Diagne, Espitia, & Karafyllis, 2022; Rathnayake, Diagne, & Karafyllis, 2022; Wang & Krstic, 2023) and hyperbolic PDEs (Espitia, 2020; Espitia et al., 2022a, 2022b, 2020; Wang & Krstic, 2021, 2022a, 2022b, 2022c; Zhang et al., 2025; Zhang & Yu, 2024), the authors have only been able to establish (global) exponential convergence of the closed-loop system to the origin, satisfying an estimate of the form

$$\Phi(t) \le Me^{-\frac{v^*t}{2}} \left( \|u[0]\|^2 + \|\hat{u}[0]\|^2 + \|v[0]\|^2 + \|\hat{v}[0]\|^2 + \|\hat{v}[0]\|^2 + m(0) \right)^{1/2},$$
(99)

for all t > 0, where  $\Phi(t)$  is given by (62), M > 0 and  $v^* > 0$  are some positive constants, and m(0) is strictly positive. Unlike the current work, where an MDT between two events is explicitly

enforced, the aforementioned works require proving the existence of an MDT since such time regularization between events is not explicitly enforced. The approach used by the authors in those works to demonstrate the existence of an MDT between events under the triggering conditions necessitates that m(0) be chosen strictly positive. This constraint prevents the authors from obtaining an exponential stabilization result as (61), (62). However, in this work, due to the use of time regularization in the triggering mechanism (45) as well as the use of switching dynamics (46), (47) for the dynamic variable m(t), we are able to choose m(0) = 0. This, along with the careful choice of the Lyapunov candidate (69)–(72) consisting of a dynamic reset variable f(t) satisfying (68), facilitates the achievement of the GES of the closed-loop system.

**Remark 4.** The closed-loop system Lyapunov candidate  $W_2(t)$ , given by (69)–(72), has been carefully chosen to ensure that it remains dissipative even though the system operates in open-loop between events. The functions  $f(t)d^2(t)$  and m(t) are employed to mitigate the effects of control input sampling, with their effects manifesting over different intervals between events, specifically  $(t_j, t_j + \tau)$  and  $(t_j + \tau, t_{j+1}), j \in \mathbb{N}$ . During the interval  $t \in (t_j, t_j + \tau)$ ,  $j \in \mathbb{N}$ , the strictly decreasing function f(t), modulated by  $d^2(t)$ , compensates for the effects of input sampling. Meanwhile, during the interval  $t \in (t_j + \tau, t_{j+1}), j \in \mathbb{N}$ , the dynamic variable m(t) compensates for these effects. In works such as Dolk and Heemels (2017), Dolk, Ploeg, and Heemels (2017), Dolk, Tesi, et al. (2017), similar Lyapunov candidates have been employed for systems described by ODEs.

The CETC design (41)–(43), (45)–(47) automatically provides an aperiodic sampled-data control approach characterized by a maximum upper diameter equal to the MDT  $\tau > 0$  of the CETC, ensuring the GES. The result is summarized in the following corollary.

**Corollary 1.** Consider a set of sampling times  $I = \{t_j\}_{j \in \mathbb{N}}$  with  $t_0 = 0$  satisfying  $\lim_{j \to \infty} t_j = +\infty$ . For every  $(u(\cdot, 0), v(\cdot, 0))^T \in L^2((0, 1); \mathbb{R}^2)$ , and  $(\hat{u}(\cdot, 0), \hat{v}(\cdot, 0))^T \in L^2((0, 1); \mathbb{R}^2)$ , there exist unique solutions  $(u, v)^T \in C^0(\mathbb{R}_{>0}; L^2((0, 1); \mathbb{R}^2))$ ,  $(\hat{u}, \hat{v})^T \in C^0(\mathbb{R}_{>0}; L^2((0, 1); \mathbb{R}^2))$ , to the systems (1)-(4), (7)-(10), (17), (18), (41)-(43). Let  $\sup_{j \ge 0} (t_{j+1} - t_j) \le \tau$ , where  $\tau > 0$  is chosen as in (57) with  $a_1, a_2 > 0$ ,  $\omega_1 > \omega_0 > 0$  being free parameters, and let  $a_0 > 0$  be chosen such that

$$a_0 = 3Cq^2 e^{\frac{\mu}{\lambda_2}} + \frac{\varepsilon_0}{a_2},\tag{100}$$

where  $\varepsilon_0 > 0$  is given by (50), subject to Assumption 1,  $\mu$  is chosen as in (51), and C > 0 is chosen such that

$$C > \max \left\{ \frac{e^{\frac{\mu}{\lambda_1}}}{1 - 3o^2 a^2 e^{\mu \left(\frac{1}{\lambda_1} + \frac{1}{\lambda_2}\right)}} \frac{\varepsilon_3}{a_2}, \frac{\max\{\varepsilon_1, \varepsilon_2\}r}{(\mu - \delta)a_2} \right\},\tag{101}$$

for some  $\delta>0$  such that  $\delta<\mu$ , and  $\varepsilon_1,\varepsilon_2,\varepsilon_3>0$  given by (54)–(56), and r defined as (53). Then, under the sampled-data boundary control (41)–(43), the closed-loop system (1)–(4), (7)–(10), (17), (18) is globally exponentially stable. More specifically, the following estimate holds:

$$\Phi(t) \le Me^{-\frac{v^*}{2}t}\Phi(0),\tag{102}$$

for some constants  $M, v^* > 0$ .

The proof follows a procedure similar to that used in the proof of Theorem 1, using the Lyapunov function (69)–(72) with  $m(t) \equiv 0$  for all  $t \geq 0$ .

#### 4. Periodic event-triggered control (PETC)

In this section, we present a triggering design that facilitates control updates only at specific events and requires only periodic evaluation of a triggering function to detect events, hence the term *periodic event-triggering*. We develop an appropriate triggering function,  $\tilde{m}(t)$ , and establish an upper bound for the sampling period h>0 used for these periodic evaluations. Periodically evaluating  $\tilde{m}(t)$  and updating the control input whenever  $\tilde{m}(t)<0$  at an evaluation time  $t=nh, n\in\mathbb{N}$  ensures that the dynamic variable m(t) governed by (46), (47) satisfies  $m(t)\geq 0$  for all t>0 along the PETC solution. This enables establishing the GES of the PETC closed-loop system, analogous to Theorem 1. Below, we present the details of the design.

**Definition 2.** Let  $\eta, \theta, \kappa_1, \kappa_2, \kappa_3, \kappa_4 > 0$  be event-trigger parameters. The set of event times  $I = \{t_j\}_{j \in \mathbb{N}}$  under PETC, which forms an increasing sequence satisfying  $\lim_{j \to \infty} t_j = +\infty$ , is defined by the following rule:

$$t_{i+1} = \inf \{ t \ge t_i + \tau \mid \tilde{m}(t) < 0, \ t = nh, \ h > 0, \ n \in \mathbb{N} \}, \quad (103)$$

where  $\tau > 0$  is the MDT to be specified, and h > 0 is a sampling period to be chosen appropriately. The function  $\tilde{m}(t)$  is defined as

$$\tilde{m}(t) := m(t) - \frac{\theta}{a} \left( e^{ah} - 1 \right) d^2(t), \tag{104}$$

where d(t) is given in (44), and m(t) satisfies (46) and (47). The constant a is defined as

$$a = 1 + \varepsilon_0 + \eta, \tag{105}$$

with  $\varepsilon_0$  given by (50).

**Theorem 2.** Consider a set of increasing event times  $I = \{t_j\}_{j \in \mathbb{N}}$  with  $t_0 = 0$ , satisfying  $\lim_{j \to \infty} t_j = +\infty$ , generated by the PETC triggering rule in Definition 2. For every  $(u(\cdot,0),v(\cdot,0))^T \in L^2((0,1);\mathbb{R}^2)$ , and  $(\hat{u}(\cdot,0),\hat{v}(\cdot,0))^T \in L^2((0,1);\mathbb{R}^2)$ , there exist unique solutions  $(u,v)^T \in C^0(\mathbb{R}_{>0};L^2((0,1);\mathbb{R}^2))$  and  $(\hat{u},\hat{v})^T \in C^0(\mathbb{R}_{>0};L^2((0,1);\mathbb{R}^2))$  to (1)-(4), (7)-(10), (17), (18), (41)-(43). Choose the event-trigger parameters  $\eta,\theta,\kappa_1,\kappa_2,\kappa_3,\kappa_4>0$  as in Assumption 2, and the MDT  $\tau>0$  as (57). Let the sampling period h>0 satisfy

$$0 < h \le \min\{\tau, \tau_1, \tau_2, \tau_3, \tau_4\}, \text{ and } \frac{\tau}{h} \in \mathbb{N}_{>0},$$
 (106)

where

$$\tau_i := \frac{1}{a} \ln \left( 1 + \frac{\kappa_i a}{\varepsilon_i \theta} \right), \quad i = 1, 2, 3, 4, \tag{107}$$

with  $\varepsilon_1$ ,  $\varepsilon_2$ ,  $\varepsilon_3$ ,  $\varepsilon_4 > 0$  given by (54)–(56), (67) and a > 0 given by (105). Further, choose the initial conditions of m(t) satisfying (46), (47) as in (58)–(60). Then, under the PETC triggering rule in Definition 2, the closed-loop system (1)–(4), (7)–(10), (17), (18), (41)–(43) is globally exponentially stable, satisfying the estimate (61), (62).

**Remark 5.** In the PETC triggering function (104), as  $h \rightarrow 0$ , we observe that

$$\tilde{m}(t) \to m(t).$$
 (108)

That is, PETC in Definition 2 converges to CETC in Definition 1 as  $h \to 0$ . This observation reveals two key insights. First, if h is very small, one can safely implement CETC on a computer by periodically checking the triggering function m(t) at intervals of length h or less to detect events. However, such a small h is generally undesirable due to the computational burden of frequent evaluations. Second, if it is possible to choose a large value for

h, PETC should be preferred over CETC, since PETC is specifically designed to require only periodic evaluations of the triggering function  $\tilde{m}(t)$  to detect events.

**Remark 6.** Although the sampling period h>0 must be chosen to be less than the MDT  $\tau>0$ , we still retain some degree of freedom in selecting h. Considering (63) under the case  $\Delta=0$ , we obtain

$$\tau = \frac{\omega_1 - \omega_0}{a_2 \left(\omega_1 + \frac{a_1}{2a_2}\right) \left(\omega_0 + \frac{a_1}{2a_2}\right)}.$$
 (109)

Instead of directly calculating the MDT  $\tau,$  we may choose any  $\tau>0$  such that

$$0 < \tau < \frac{1}{a_2 \left(\omega_0 + \frac{a_1}{2a_2}\right)},\tag{110}$$

and then compute  $\omega_1 > \omega_0$  using (109) as

$$\omega_1 = \frac{\omega_0 + \frac{\tau a_1}{2} \left(\omega_0 + \frac{a_1}{2a_2}\right)}{1 - \tau a_2 \left(\omega_0 + \frac{a_1}{2a_2}\right)}.$$
(111)

Therefore, we have some flexibility in selecting the MDT  $\tau > 0$  and, consequently, the sampling period h > 0.

In the following subsection, we complete the proof of Theorem 2.

## 4.1. Proof of Theorem 2

#### 4.1.1. Preliminaries

Before proceeding to the proof of Theorem 2, we provide several necessary auxiliary results below in Lemmas 4 and 5.

**Lemma 4.** Consider a set of increasing event times  $I = \{t_j\}_{j \in \mathbb{N}}$  with  $t_0 = 0$  satisfying  $\lim_{j \to \infty} t_j = +\infty$ , generated by the PETC triggering rule in Definition 2. Also, consider the dynamic variable m(t) governed by (46), (47) with  $m(t_0) = 0$ ,  $m(t_j) \ge 0$ ,  $j \in \mathbb{N}_{>0}$  to be chosen, and  $m((t_j + \tau)^-) = m(t_j + \tau)$ ,  $j \in \mathbb{N}$  for any  $\tau > 0$ . Then, it holds that  $m(t) \ge 0$  for all  $t \in (t_j, t_j + \tau]$ ,  $j \in \mathbb{N}$ . Choose the sampling period h > 0 as in (106), (107). Then, it holds that

$$m(t) \ge \frac{\theta}{a} \left( \frac{a}{\theta} m(nh) - \left( e^{a(t-nh)} - 1 \right) d^2(nh) \right) e^{-\eta(t-nh)}, \tag{112}$$

for all  $t \in [nh, (n+1)h)$  and  $n \in [(t_j + \tau)/h, t_{j+1}/h) \cap \mathbb{N}$ , where d(t) is given by (44).

**Proof.** If  $m(t_0) = 0$ ,  $m(t_j) \ge 0$ ,  $j \in \mathbb{N}_{>0}$  to be chosen, and  $m((t_j + \tau)^-) = m(t_j + \tau)$ ,  $j \in \mathbb{N}$ , using similar arguments used in the proof of Lemma 1, it can be shown that  $m(t) \ge 0$  for all  $t \in (t_i, t_i + \tau]$ ,  $j \in \mathbb{N}$ .

For all  $t \in (nh, (n+1)h)$  and  $n \in [(t_j + \tau)/h, t_{j+1}/h) \cap \mathbb{N}$ , using Young's inequality and considering (66), we can write that

$$(d^{2}(t)) = 2d(t)\dot{d}(t) \leq d^{2}(t) + (\dot{d}(t))^{2}$$

$$\leq (1 + \varepsilon_{0})d^{2}(t) + \varepsilon_{1}\|\hat{\alpha}[t]\|^{2} + \varepsilon_{2}\|\hat{\beta}[t]\|^{2}$$

$$+ \varepsilon_{3}\hat{\alpha}^{2}(1, t) + \varepsilon_{4}\tilde{\alpha}^{2}(1, t).$$
(113)

Since the both sides of the inequality (113) are well-behaved, there exists  $\iota(t) > 0$  such that

$$(d^{2}(t)) = (1 + \varepsilon_{0})d^{2}(t) + \varepsilon_{1}\|\hat{\alpha}[t]\|^{2} + \varepsilon_{2}\|\hat{\beta}[t]\|^{2} + \varepsilon_{3}\hat{\alpha}^{2}(1, t) + \varepsilon_{4}\tilde{\alpha}^{2}(1, t) - \iota(t),$$

$$(114)$$

for all  $t \in (nh, (n+1)h)$  and  $n \in [(t_j+\tau)/h, t_{j+1}/h) \cap \mathbb{N}$ . Combining (47) and (114), we can write the following system valid for all  $t \in (nh, (n+1)h)$  and  $n \in [(t_i+\tau)/h, t_{j+1}/h) \cap \mathbb{N}$ 

$$\dot{z}(t) = \mathcal{A}z(t) + \psi(t), \tag{115}$$

where

$$z(t) = \begin{bmatrix} m(t) \\ d^{2}(t) \end{bmatrix}, \ A = \begin{bmatrix} -\eta & -\theta \\ 0 & 1 + \varepsilon_{0} \end{bmatrix},$$

$$\psi(t) = \begin{bmatrix} \kappa_{1} \|\hat{\alpha}[t]\|^{2} + \kappa_{2} \|\hat{\beta}[t]\|^{2} + \kappa_{3}\hat{\alpha}^{2}(1, t) + \kappa_{4}\tilde{\alpha}^{2}(1, t) \\ \varepsilon_{1} \|\hat{\alpha}[t]\|^{2} + \varepsilon_{2} \|\hat{\beta}[t]\|^{2} + \varepsilon_{3}\hat{\alpha}^{2}(1, t) + \varepsilon_{4}\tilde{\alpha}^{2}(1, t) - \iota(t) \end{bmatrix}.$$
(116)

Thus, from (115), we can obtain that

$$z(t) = e^{\mathcal{A}(t-nh)}z(nh) + \int_{nh}^{t} e^{\mathcal{A}(t-\xi)}\psi(\xi)d\xi, \qquad (117)$$

for all  $t \in [nh, (n+1)h)$  and  $n \in [(t_j + \tau)/h, t_{j+1}/h) \cap \mathbb{N}$ , from which it follows that

$$m(t) = Re^{\mathcal{A}(t-nh)}z(nh) + \int_{rh}^{t} Re^{\mathcal{A}(t-\xi)}\psi(\xi)d\xi, \qquad (118)$$

for all  $t \in [nh, (n+1)h)$  and  $n \in [(t_j + \tau)/h, t_{j+1}/h) \cap \mathbb{N}$ , where

$$R = \begin{bmatrix} 1 & 0 \end{bmatrix}. \tag{119}$$

The eigenvalues of  $\mathcal{A}$  are  $-\eta$  and  $1 + \varepsilon_0$ . Using matrix diagonalization,  $e^{\mathcal{A}t}$  can be obtained as

$$e^{\mathcal{A}t} = \begin{bmatrix} 1 & -\frac{\theta}{a} \\ 0 & 1 \end{bmatrix} \begin{bmatrix} e^{-\eta t} & 0 \\ 0 & e^{(1+\varepsilon_0)t} \end{bmatrix} \begin{bmatrix} 1 & \frac{\theta}{a} \\ 0 & 1 \end{bmatrix}, \tag{120}$$

where a is given by (105). Therefore, we can show that

$$Re^{\mathcal{A}(t-\xi)}\psi(\xi) = \left(\kappa_{1}g_{1}(t-\xi) - \varepsilon_{1}g_{2}(t-\xi)\right) \|\hat{\alpha}[\xi]\|^{2}$$

$$+ \left(\kappa_{2}g_{1}(t-\xi) - \varepsilon_{2}g_{2}(t-\xi)\right) \|\hat{\beta}[\xi]\|^{2}$$

$$+ \left(\kappa_{3}g_{1}(t-\xi) - \varepsilon_{3}g_{2}(t-\xi)\right) \hat{\alpha}^{2}(1,\xi)$$

$$+ \left(\kappa_{4}g_{1}(t-\xi) - \varepsilon_{4}g_{2}(t-\xi)\right) \tilde{\alpha}^{2}(1,\xi)$$

$$+ g_{2}(t-\xi)\iota(\xi).$$

$$(121)$$

where

$$g_1(t) = e^{-\eta t} \ge 0,$$
 (122)

and

$$g_2(t) = \frac{\theta}{a} (e^{at} - 1)e^{-\eta t} \ge 0. \tag{123}$$

Considering (122) and (123), recalling that  $nh \le \xi \le t < (n+1)h$ , and that h > 0 has been chosen as in (106), (107), it can be shown that

$$\kappa_{i}g_{1}(t-\xi) - \varepsilon_{i}g_{2}(t-\xi) = \frac{\varepsilon_{i}\theta}{a} \left( 1 + \frac{\kappa_{i}a}{\varepsilon_{i}\theta} - e^{a(t-\xi)} \right) e^{-\eta(t-\xi)} \\
\geq \frac{\varepsilon_{i}\theta}{a} \left( 1 + \frac{\kappa_{i}a}{\varepsilon_{i}\theta} - e^{ah} \right) e^{-\eta h} \geq 0, \tag{124}$$

for i = 1, 2, 3, 4. Thus, it follows from (121) that

$$Re^{\mathcal{A}(t-\xi)}\psi(\xi) \ge 0,$$
 (125)

for all  $t, \xi$  such that  $nh \leq \xi \leq t < (n+1)h$ , and  $n \in [(t_j + \tau)/h, t_{j+1}/h) \cap \mathbb{N}$ . Therefore, considering (118)–(120), (125), it can be shown that

$$m(t) \ge Re^{A(t-nh)}z(nh)$$

$$= \frac{\theta}{a} \left( \frac{a}{\theta} m(nh) - \left( e^{a(t-nh)} - 1 \right) d^2(nh) \right) e^{-\eta(t-nh)}. \tag{126}$$

for all  $t \in [nh, (n+1)h)$  and  $n \in [(t_j + \tau)/h, t_{j+1}/h) \cap \mathbb{N}$ . This completes the proof.

**Lemma 5.** Consider a set of increasing event times  $I = \{t_j\}_{j \in \mathbb{N}}$  with  $t_0 = 0$  satisfying  $\lim_{j \to \infty} t_j = +\infty$ , generated by the PETC triggering rule in Definition 2. Also consider the dynamic variable m(t) governed by (46), (47) with  $m(t_0) = 0$ ,  $m(t_j) \ge 0$ ,  $j \in \mathbb{N}_{>0}$  to be chosen, and  $m((t_j + \tau)^-) = m(t_j + \tau)$ ,  $j \in \mathbb{N}$ , for any  $\tau > 0$ . Let the sampling period h > 0 be chosen as in (106), (107). Then, it holds that  $m(t) \ge 0$  for all t > 0.

**Proof.** Let us assume an event has triggered at  $t=t_j$  and  $m(t_j)\geq 0, j\in\mathbb{N}$ . Then, it follows from Lemma 4 that  $m(t)\geq 0$  for all  $t\in (t_j,t_j+\tau], j\in\mathbb{N}$ . At every t=nh, the periodic event-trigger (103)-(105) is evaluated, leading to an event trigger only if  $t\geq t_j+\tau$  and  $\tilde{m}(nh)<0$ ,i.e.,  $m(nh)<\frac{\theta}{a}(e^{ah}-1)d^2(nh)$ , necessitating a control update. In cases when  $t\geq t_j+\tau$  and  $\tilde{m}(nh)\geq 0$ , i.e.,  $m(nh)\geq \frac{\theta}{a}(e^{ah}-1)d^2(nh)$ , an update is not required as it holds that  $m(t)\geq 0$  for all  $t\in [nh,(n+1)h)$ . This is because the RHS of (112) is definitely non-negative when  $m(nh)\geq \frac{\theta}{a}(e^{ah}-1)d^2(nh)$ . Thus, m(t) will remain non-negative at least until  $t=t_{j+1}$  when  $\tilde{m}(t_{j+1})<0$ , i.e.,  $m(t_{j+1})<\frac{\theta}{a}(e^{ah}-1)d^2(t_{j+1})$ , at which the control input is updated, and  $m(t_{j+1})\geq 0$  is chosen. Therefore, if  $m(t_0)=0$  and  $m(t_j)\geq 0$ ,  $j\in\mathbb{N}$ , it holds that  $m(t)\geq 0$  for all  $t\in (t_j+\tau,t_{j+1})$ ,  $j\in\mathbb{N}$ , implying that  $m(t)\geq 0$  for all t>0. This completes the proof.

#### 4.1.2. Main proof

With Proposition 1 and Lemmas 4 and 5 in hand, we are now in a position to proceed with the proof of Theorem 2.

The well-posedness in the sense of Theorem 2 is obtained by applying Proposition 1 iteratively in between events.

Since the initial conditions of m(t) are chosen as (58)–(60) and the sampling period h>0 is chosen as in (106), (107), it follows from Lemma 5 that  $m(t)\geq 0$  for all t>0. Furthermore, since the MDT  $\tau>0$  is chosen as in (57), it follows from Lemma 3 that for the function f(t) satisfying (68), with  $f(t_j)=\omega_1>0$  and  $f\left((t_j+\tau)^-\right)=f(t_j+\tau)=\omega_0>0$  for all  $j\in\mathbb{N}$ , we have f(t)>0 for all t>0. Thus, we can follow the same proof procedure as in the proof of Theorem 1, using the Lyapunov candidate (69)–(73), to establish the GES of the closed-loop system under the PETC approach. The only difference is that as opposed to (92) where  $m(t_j^-)=0$ , under PETC, it holds that

$$W_2(t_i^-) = W_1(t_i) + \omega_0 d^2(t_i^-) + m(t_i^-), \tag{127}$$

where  $m(t_j^-) \ge 0$  (see Lemma 5). However, since  $m(t_j)$  is chosen as (60) and that  $d(t_i) = 0$ , we have that

$$W_2(t_j) = W_1(t_j) + \omega_0 d^2(t_i^-) \le W_2(t_i^-). \tag{128}$$

Then, using similar arguments to those used in (95)–(98), the GES of the closed-loop system is obtained. This completes the proof of Theorem 2.

# 5. Self-triggered control (STC)

In this section, we consider the full-state feedback problem only. Thus, dismissing the observer-induced effects in Section 2, we write the full-state feedback sampled-data control input as

$$U(t_j) := U_j = \int_0^1 N^{\alpha}(y)\alpha(y, t_j)dy + \int_0^1 N^{\beta}(y)\beta(y, t_j)dy,$$
 (129)

for all  $t \in [t_j, t_{j+1}), j \in \mathbb{N}$ , where  $N^{\alpha}$ ,  $N^{\beta}$  are given by (42), (43), and  $(\alpha, \beta)$  satisfies

$$\alpha_t(x, t) + \lambda_1 \alpha_x(x, t) = 0, \ \forall x \in (0, 1),$$
 (130)

$$\beta_t(x,t) - \lambda_2 \beta_x(x,t) = 0, \ \forall x \in (0,1),$$
 (131)

$$\alpha(0,t) = q\beta(0,t),\tag{132}$$

$$\beta(1,t) = \rho \alpha(1,t) + d(t), \tag{133}$$

for all  $t \in (t_j, t_{j+1}), j \in \mathbb{N}$ , with d(t) being the control input sampling error given by

$$d(t) = \int_0^1 N^{\alpha}(y) (\alpha(y, t_j) - \alpha(y, t)) dy$$

$$+ \int_0^1 N^{\beta}(y) (\beta(y, t_j) - \beta(y, t)) dy,$$
(134)

for all  $t \in (t_j, t_{j+1}), j \in \mathbb{N}$ . We design a self-triggering mechanism to determine the control update times.

**Assumption 3.** The reflection terms are small enough such that the following inequality holds:

$$|\rho q| < \frac{1}{\sqrt{2}}.\tag{135}$$

Note that Assumption 3 is less restrictive than Assumption 1. Below we present the details of STC.

**Definition 3.** Let  $\eta, \theta, \mu, \omega_0 > 0$  be self-trigger parameters. The set of event times  $I = \{t_j\}_{j \in \mathbb{N}}$  under STC, which forms an increasing sequence satisfying  $\lim_{j \to \infty} t_j = +\infty$ , is defined by the following rule:

$$t_{1} = t_{0} + \tau,$$

$$t_{j+1} = t_{j} + \tau$$

$$+ \frac{1}{\varrho^{\star} + \eta} \ln \left( 1 + \frac{(\varrho^{\star} + \eta)\omega_{0}(U_{j} - U_{j-1})^{2}}{\theta e^{(\varrho^{\star} + \eta)\tau} (H(\alpha[t_{i}], \beta[t_{i}]) + \epsilon)} \right),$$

$$(136)$$

for  $j \in \mathbb{N}_{>0}$ , where  $\tau > 0$  is the MDT to be set,  $\epsilon > 0$ ,  $U_j, j \in \mathbb{N}$  given by (129) is the control input updated at  $t = t_i$ ,

$$\varrho^{\star} := 2q^2 e^{\frac{\mu}{\lambda_2}} \varrho, \tag{137}$$

$$H(\alpha[t], \beta[t])$$

$$:= 3\varrho \int_0^1 \left( \frac{1}{\lambda_1} \alpha^2(x, t) e^{-\frac{\mu x}{\lambda_1}} + \frac{q^2}{\lambda_2} \beta^2(x, t) e^{\frac{\mu x}{\lambda_2}} \right) dx,$$
(138)

with

$$\varrho = 4 \max \left\{ \lambda_1 \| N^{\alpha} \|^2 e^{\frac{\mu}{\lambda_1}}, \frac{\lambda_2}{q^2} \| N^{\beta} \|^2 \right\}.$$
 (139)

In (139),  $N^{\alpha}$  and  $N^{\beta}$  are given by (42), (43). Further, in (136), (138),  $\alpha[t]$ ,  $\beta[t]$  are given by

$$\alpha(x,t) = u(x,t) - \int_0^x K^{uu}(x,y)u(y,t)dy - \int_0^x K^{uv}(x,y)v(y,t)dy,$$
(140)

$$\beta(x,t) = v(x,t) - \int_0^x K^{vu}(x,y)u(y,t)dy - \int_0^x K^{vv}(x,y)v(y,t)dy,$$
(141)

where  $K^{uu}$ ,  $K^{uv}$ ,  $K^{vu}$ ,  $K^{vv}$  are the backstepping gain kernels defined in the triangular domain  $0 \le y \le x \le 1$ . The readers are referred to Vazquez et al. (2011) for details on these gain kernels.

**Remark 7.** CETC in Definition 1 continuously monitors a triggering function to detect events, whereas PETC in Definition 2, monitors a triggering function only *periodically*. Due to the

involvement of the dynamic variable m(t) satisfying (46), (47), in both CETC and PETC triggering functions, both schemes even in the full-state feedback case require continuous measurements from the plant in order to compute and evolve the dynamic variable m(t). In contrast, STC in Definition 3 requires neither continuous monitoring of a triggering function nor continuous measurements from the plant. At each event time, the STC triggering rule (136) computes the next event time using only the measurements obtained at the current event and the immediate previous event. In this sense, we refer to the STC design as relying solely on event-triggered measurements, in contrast to CETC and PETC, which rely on continuous measurements.

**Assumption 4** (*Self-trigger Parameter Selection*). The parameters  $\eta, \omega_0 > 0$  are free parameters. Subject to Assumption 3, the parameter  $\mu > 0$  is chosen such that

$$0 < \mu < \frac{\lambda_1 \lambda_2}{\lambda_1 + \lambda_2} \ln \left( \frac{1}{2\rho^2 q^2} \right). \tag{142}$$

Furthermore, the parameter  $\theta > 0$  is chosen as

$$\theta = a_2 \omega_0^2 + a_1 \omega_0 + a_0, \tag{143}$$

where  $a_1, a_2 > 0$ , and

$$a_0 = 2Cq^2 e^{\frac{\mu}{\lambda_2}} + \frac{\varepsilon_0}{a_2}. (144)$$

Here

$$\varepsilon_0 = 4\lambda_2^2 \left( N^{\beta}(1) \right)^2, \tag{145}$$

where  $N^{\beta}(y)$  is given in (43), and C > 0 is chosen to satisfy

$$C > \max \left\{ \frac{e^{\frac{\mu}{\lambda_1}}}{1 - 2\rho^2 q^2 e^{\mu\left(\frac{1}{\lambda_1} + \frac{1}{\lambda_2}\right)}} \left(\frac{\varepsilon_3}{a_2} + \kappa_3\right), \\ \frac{1}{\mu} \left(\frac{\max\{\varepsilon_1, \varepsilon_2\}r}{a_2} + \max\{\kappa_1, \kappa_2\}r\right) \right\},$$
 (146)

for some constants  $\kappa_1, \kappa_2, \kappa_3 > 0$  with r given by (53). Moreover,

$$\varepsilon_1 = 4\lambda_1^2 \int_0^1 \left( \dot{N}^{\alpha}(y) \right)^2 dy, \tag{147}$$

$$\varepsilon_2 = 4\lambda_2^2 \int_0^1 \left( \dot{N}^{\beta}(y) \right)^2 dy, \tag{148}$$

$$\varepsilon_3 = 4 \left( \lambda_1 N^{\alpha}(1) - \rho \lambda_2 N^{\beta}(1) \right)^2, \tag{149}$$

where  $N^{\alpha}(y)$  is given in (42).

**Theorem 3.** Consider a set of increasing event times  $I = \{t_j\}_{j \in \mathbb{N}}$  with  $t_0 = 0$ , satisfying  $\lim_{j \to \infty} t_j = +\infty$ , generated by the STC triggering rule in Definition 3. For every  $(u(\cdot,0),v(\cdot,0))^T \in L^2((0,1);\mathbb{R}^2)$ , there exists a unique solution  $(u,v)^T \in C^0(\mathbb{R}_{>0};L^2((0,1);\mathbb{R}^2))$  to the system (1)–(4), (129). Choose the self-trigger parameters  $\eta,\theta,\mu,\omega_0>0$  as outlined in Assumption 4 and the MDT  $\tau>0$  as

$$\tau = \int_{\omega_0}^{\omega_1} \frac{1}{a_2 s^2 + a_1 s + a_0} ds,\tag{150}$$

where  $a_1, a_2 > 0$ ,  $\omega_1 > \omega_0 > 0$ , and  $a_0 > 0$  is chosen as (144). Then, under the STC triggering rule in Definition 3, the closed-loop system (1)–(4), (129) is globally exponentially stable. More specifically, the following estimate holds:

$$\Phi(t) \le M_{\text{stc}} e^{-\frac{v_{\text{stc}}^*}{2}t} \Phi(0), \tag{151}$$

for all t>0, where  $\Phi(t)=\|u[t]\|+\|v[t]\|$ , for some constants  $M_{\rm stc}, \upsilon_{\rm stc}^{\star}>0$ .

#### 5.1. Proof of Theorem 3

#### 5.1.1. Preliminaries

Before proceeding to the proof of Theorem 3, we provide several necessary auxiliary results below in Lemmas 6 and 7.

**Lemma 6.** Consider a set of increasing event times  $I = \{t_j\}_{j \in \mathbb{N}}$  with  $t_0 = 0$ , satisfying  $\lim_{j \to \infty} t_j = +\infty$ , generated by the STC triggering rule in Definition 3. Then, under Assumption 3, if the self-trigger parameter  $\mu > 0$  is chosen as in (142), the control input sampling error d(t), given by (134), satisfies the following estimate for all  $t \in [t_i, t_{i+1}], j \in \mathbb{N}$ :

$$d^{2}(t) \leq H(\alpha[t_{i}], \beta[t_{i}])e^{\varrho^{\star}(t-t_{i})}, \tag{152}$$

where  $H(\cdot, \cdot)$  is given by (138), (139), and  $\varrho^* > 0$  is given by (137), (139).

The proof follows similar steps to that of Lemma 6 of Zhang et al. (2025).

**Lemma 7.** Consider a set of increasing event times  $I = \{t_j\}_{j \in \mathbb{N}}$  with  $t_0 = 0$ , satisfying  $\lim_{j \to \infty} t_j = +\infty$ , generated by the STC triggering rule in Definition 3. Furthermore, consider a dynamic variable m(t) that satisfies

$$\dot{m}(t) = -\eta m(t) + \kappa_1 \|\alpha[t]\|^2 + \kappa_2 \|\beta[t]\|^2 + \kappa_3 \alpha^2(1, t), \tag{153}$$

for all  $t \in (t_i, t_i + \tau)$ ,  $j \in \mathbb{N}$ , and

$$\dot{m}(t) = -\eta m(t) - \theta d^{2}(t) + \kappa_{1} \|\alpha[t]\|^{2} + \kappa_{2} \|\beta[t]\|^{2} + \kappa_{3} \alpha^{2}(1, t),$$
(154)

for all  $t \in (t_j + \tau, t_{j+1})$ ,  $j \in \mathbb{N}$ , with  $m(t_0) = m(0) = 0$ ,  $m((t_j + \tau)^-) = m(t_j + \tau)$  for any  $\tau > 0$ , and  $m(t_j)$  for  $j \in \mathbb{N}_{>0}$  defined as  $m(t_j) = \omega_0(U_j - U_{j-1})^2$ , where  $U_j$ ,  $j \in \mathbb{N}$ , is the control input updated at  $t = t_j$  as given by (129). Assume that  $\eta, \theta, \kappa_1, \kappa_2, \kappa_3 > 0$ . In (154), d(t) is defined by (134). If the self-trigger parameter  $\mu > 0$  is chosen according to (142), then it holds that  $m(t) \geq 0$  for all t > 0.

**Proof.** Considering (153), we obtain that

$$m(t) = e^{-\eta(t-t_{j})} m(t_{j}) + \int_{t_{j}}^{t} e^{-\eta(t-\xi)} \left( \kappa_{1} \|\alpha[\xi]\|^{2} + \kappa_{2} \|\beta[\xi]\|^{2} + \kappa_{3} \alpha^{2}(1,\xi) \right) d\xi$$

$$> e^{-\eta(t-t_{j})} m(t_{i}).$$
(155)

for all  $t \in (t_j, t_j + \tau], j \in \mathbb{N}$ . If  $m(t_j)$  is chosen  $m(t_j) \ge 0$ , it follows that  $m(t) \ge 0$  for all  $t \in (t_j, t_j + \tau], j \in \mathbb{N}$ .

Now consider the time period when  $t \in (t_j + \tau, t_{j+1}), j \in \mathbb{N}_{>0}$ . Recalling (152) from Lemma 6 and considering (154), we obtain that

$$\dot{m}(t) \ge -\eta m(t) - \theta H(\alpha[t_i], \beta[t_i]) e^{\rho^*(t-t_i)}, \tag{156}$$

from which it follows that

$$m(t) \geq m(t_i + \tau)e^{-\eta(t-t_j-\tau)}$$

$$-\frac{\theta H(\alpha[t_j], \beta[t_j])e^{\varrho^{\star}\tau}}{\rho^{\star} + \eta}e^{-\eta(t-t_j-\tau)}\left(e^{(\varrho^{\star} + \eta)(t-t_j-\tau)} - 1\right), \tag{157}$$

for all  $t \in [t_j + \tau, t_{j+1}), j \in \mathbb{N}_{>0}$ . Then, noting from (155) that  $m(t_j + \tau) \ge e^{-\eta \tau} m(t_j)$ , we obtain

$$m(t) \ge m(t_j)e^{-\eta\tau}e^{-\eta(t-t_j-\tau)} - \frac{\theta H(\alpha[t_j], \beta[t_j])e^{\rho^{\star}\tau}}{\rho^{\star} + \eta}e^{-\eta(t-t_j-\tau)} \left(e^{(\rho^{\star} + \eta)(t-t_j-\tau)} - 1\right),$$
(158)

for all  $t \in [t_i + \tau, t_{i+1}), j \in \mathbb{N}_{>0}$ . Then, it directly follows that

$$m(t) \ge e^{-\eta(t-t_{j}-\tau)} \left\{ m(t_{j})e^{-\eta\tau} - \frac{\theta H(\alpha[t_{j}], \beta[t_{j}])e^{\varrho^{\star}\tau}}{\varrho^{\star} + \eta} \left( e^{(\varrho^{\star} + \eta)(t_{j+1} - t_{j} - \tau)} - 1 \right) \right\},$$

$$(159)$$

for all  $t \in [t_j + \tau, t_{j+1}), j \in \mathbb{N}_{>0}$ . Then, recalling that  $m(t_j)$  is chosen as  $m(t_j) = \omega_0 (U_j - U_{j-1})^2$  for  $j \in \mathbb{N}_{>0}$  and that events are triggered according to (136), we have that

$$m(t) \ge e^{-\eta(t-t_j)} \frac{\omega_0 (U_j - U_{j-1})^2 \epsilon}{H(\alpha[t_i], \beta[t_i]) + \epsilon} \ge 0, \tag{160}$$

for all  $t \in [t_j + \tau, t_{j+1}), j \in \mathbb{N}_{>0}$ . Therefore, we can conclude that m(t) > 0 for all t > 0.

## 5.1.2. Main proof

The well-posedness in the sense of Theorem 3 is obtained by iteratively applying the results of Proposition 1 in between events.

Let the initial conditions of m(t) governed by (153), (154) be chosen as

$$m(t_0) = m(0) = 0,$$
 (161)

$$m((t_j + \tau)^-) = m(t_j + \tau), \text{ for } j \in \mathbb{N},$$
(162)

$$m(t_j) = \omega_0 (U_j - U_{j-1})^2 = \omega_0 d^2(t_i^-), \text{ for } j \in \mathbb{N}_{>0},$$
(163)

where d(t) is given by (134). Then, it follows from Lemma 7 that m(t) satisfies m(t) > 0 for all t > 0.

Let us consider the following Lyapunov candidate

$$W_2(t) = W_1(t) + f(t)d^2(t) + m(t), (164)$$

where f(t) satisfies (68), d(t) is given by (134), m(t) satisfies (153), (154), and  $W_1(t)$  is given by

$$W_1(t) = \int_0^1 \left( \frac{C}{\lambda_1} \alpha^2(x, t) e^{-\frac{\mu x}{\lambda_1}} + \frac{D}{\lambda_2} \beta^2(x, t) e^{\frac{\mu x}{\lambda_2}} \right) dx, \tag{165}$$

with  $(\alpha, \beta)$  satisfying (130)–(133),  $\mu > 0$  chosen as in (142), C > 0 chosen as in (146), and  $D = Cq^2$ . Recall from Lemma 3 that f(t) > 0 for all t > 0 if the MDT  $\tau > 0$  is chosen as (150).

Then, we can follow a procedure very similar to the one presented in the proof of Theorem 1, with the differences outlined in the proof of Theorem 2, to show that

$$W_1(t) < e^{-v_{\text{stc}}^* t} W_1(0), \tag{166}$$

for all t > 0, where

$$\upsilon_{\text{stc}}^{\star} := \min\{\upsilon_{\text{stc}}, a_1, \eta\},\tag{167}$$

with

$$\upsilon_{\text{stc}} := \mu - \frac{\max\{\varepsilon_1, \varepsilon_2\}r}{Ca_2} - \frac{\max\{\kappa_1, \kappa_2\}r}{C},\tag{168}$$

from which it follows the GES of the closed-loop system satisfying (151). This completes the proof of Theorem 3.  $\Box$ 

#### 6. Numerical simulations

We consider the system (1)–(4) with plant parameters  $\lambda_1=1$ ,  $\lambda_2=1$ ,  $c_1(x)=1$ , and  $c_2(x)=1.5$  for all  $x\in(0,1)$ , and q=0.5. We select  $\rho=0$  to satisfy Assumption 1. The initial conditions are selected as  $u^0(x)=qv^0(x)$ , with  $v^0(x)=10(1-x)$ . For both CETC and PETC, we consider the observer-based problem, where the

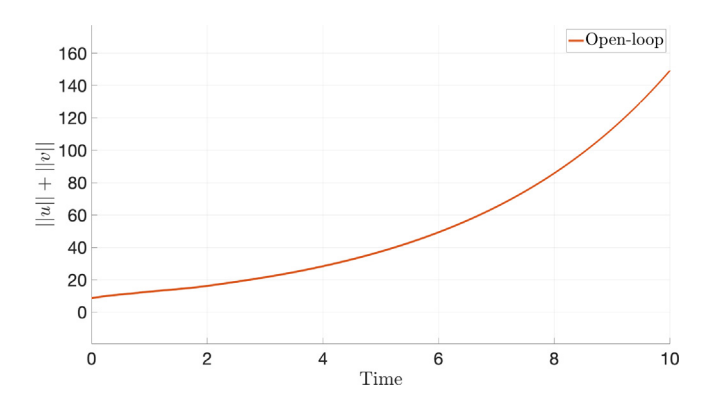


**Fig. 3.** Evolution of  $L^2$  norms of states with no control (open-loop).

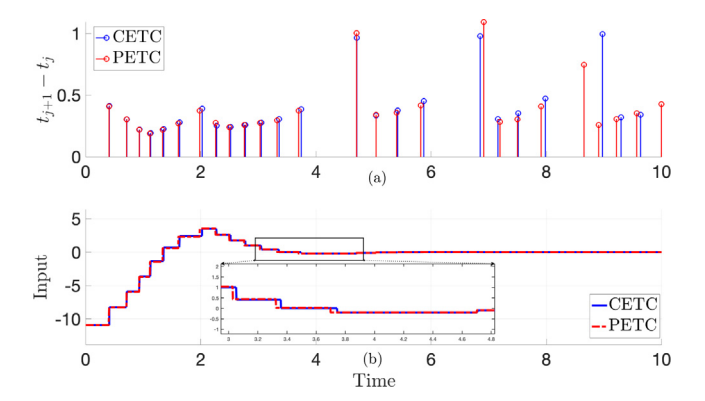


Fig. 4. (a) Dwell-times under CETC and PETC. (b) CETC and PETC inputs.

initial conditions for the observer are chosen as  $\hat{u}^0(x) = 1.5u^0(x)$  and  $\hat{v}^0(x) = 1.5v^0(x)$  for all  $x \in (0, 1)$ . Note that the chosen plant parameters satisfy the condition (6), and hence, the open-loop system is unstable. In Fig. 3, we show the evolution of the  $L^2$  norm of the states of the open-loop system, where it is evident that the system is unstable.

#### 6.1. CETC and PETC

The parameters for the CETC and PETC triggering mechanisms are chosen as follows: The parameters  $\kappa_i$ 's,  $\eta$ ,  $a_2$ ,  $\omega_0$ ,  $\omega_1$  are chosen as  $\kappa_i=1$ , i=1,2,3,4,  $\eta=1$ ,  $a_2=1$ ,  $\omega_0=1$ , and  $\omega_1=10$ . It can be shown using (50)–(67) that  $\varepsilon_0=6.3281$ ,  $\varepsilon_1=0.7302$ ,  $\varepsilon_2=1.7823$ ,  $\varepsilon_3=2.8125$ ,  $\varepsilon_4=20.3216$ . The parameter  $\mu$  is chosen as  $\mu=1$  such that (51) is satisfied,  $\delta<\mu$  is chosen as  $\delta=0.5$ , and  $\delta=0.5$ , and and an is chosen as  $\delta=0.5$ , and an is calculated that an another computed MDT is 0.0640. Thus, we use  $\delta=0.0001$  to time discretize the plant and observer dynamics. Following (106), we choose  $\delta=0.0032$  as the sampling period for the PETC approach. Space discretization is done using a step size of  $\delta=0.005$ .

In Figs. 4 and 5, we present results for both observer-based CETC and PETC. Fig. 4(a) illustrates the dwell-times, while Fig. 4(b) shows the CETC and PETC inputs. Fig. 5(a) depicts the evolution of the  $L^2$  norms under CETC and PETC, which closely follow each other. Finally, Fig. 5(b) shows the evolution of the  $L^2$  norms of the observer error under CETC and PETC, where the two trajectories are identical because the observer error system (13)–(16) is independent of the control input.

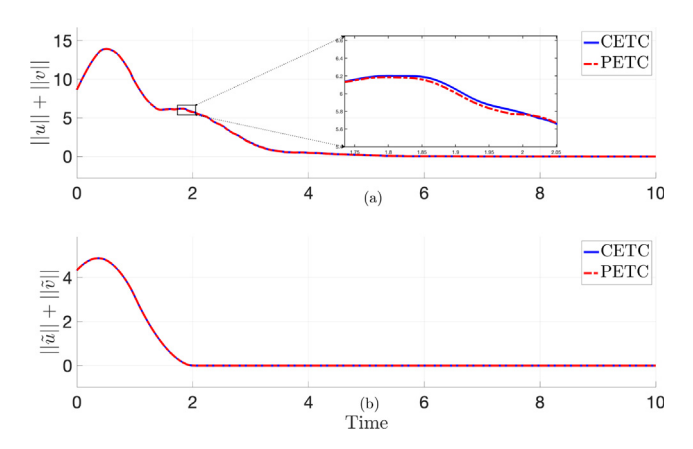


**Fig. 5.** (a)  $L^2$  norms of states under CETC and PETC. (b)  $L^2$  norms of observer errors under CETC and PETC.

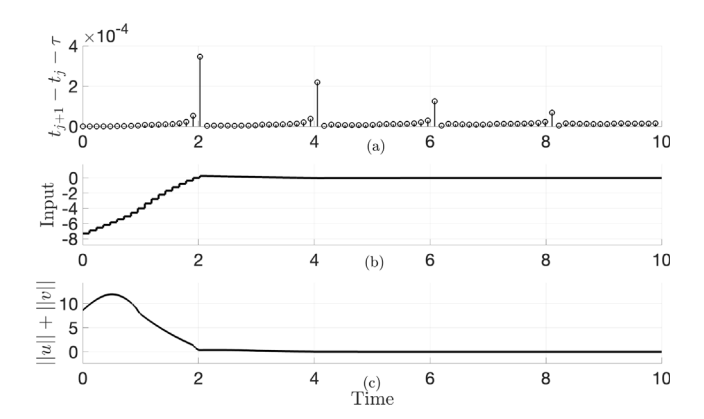


**Fig. 6.** Results under STC. (a)  $t_{j+1}-t_j-\tau$ . (b) Control input. (c)  $L^2$  norm of states

#### 6.2. STC

The parameters for the STC triggering mechanism are chosen as follows: The parameters  $\kappa_i$ 's,  $\eta$ ,  $a_2$ ,  $\omega_0$ ,  $\omega_1$  are chosen as  $\kappa_i=1,i=1,2,3,\ \eta=1,a_2=1,\omega_0=1,$  and  $\omega_1=10.$  It can be shown using (145), (147)–(149) that  $\varepsilon_0=5.0625, \varepsilon_1=0.5841, \varepsilon_2=1.4258, \varepsilon_3=2.2500.$  The parameter  $\mu$  is chosen as  $\mu=1$  such that (142) is satisfied, and C>0 is chosen as C=9.8032 such that (146) is satisfied. Then, using (144), it is calculated that  $a_0=18.3865,$  and  $a_1$  is chosen as  $a_1=2\sqrt{a_0a_2}=8.5759.$  Using (143),  $\theta$  is calculated to be  $\theta=27.9624.$  The computed MDT is 0.1191. Thus, we use  $\Delta t=0.0001$  to time discretize the plant dynamics. Space discretization is done using a step size of  $\Delta x=0.005.$ 

In Fig. 6, we present results for full-state feedback STC. Fig. 6(a) illustrates the value of  $t_{j+1}-t_j-\tau$  satisfying (136), while Fig. 6(b) shows the STC inputs. Although the events are triggered aperiodically, due to the conservativeness of STC — stemming from not monitoring any triggering conditions and relying solely on event-triggered measurements — the events appear to be almost periodic, with a period of  $\tau$ . Fig. 6(c) depicts the evolution of the  $L^2$  norms of states under STC.

#### 7. Conclusions

In this paper, we have introduced novel dynamic event-triggered control (ETC) mechanisms — continuous-time event-triggered control (CETC), periodic event-triggered control (PETC), and self-triggered control (STC) — for  $2 \times 2$  linear hyperbolic PDEs

using PDE backstepping. Our designs achieve global exponential stability (GES) under ETC, marking a significant advancement over previous works based on PDE backstepping with dynamic eventtriggering, which have only established exponential convergence. The CETC design introduces a switching dynamic variable and enforces a minimal dwell-time between events, ensuring GES while requiring continuous monitoring of a triggering condition. The PETC approach overcomes the need for continuous monitoring by periodically checking an appropriate triggering condition, while still retaining the GES property. The STC design, in addition to not requiring any monitoring of a triggering condition, further advances the state of the art by eliminating the need for continuous measurements in triggering, while still delivering GES. Though conservative, it computes the next event time at the current event using only event-triggered full-state measurements, a feature not previously achieved in ETC with PDE backstepping, which required continuous measurements for the triggering mechanism. One possible direction to mitigate the conservatism of STC is to integrate the performance-barrier ETC concept, as explored in Rathnayake et al. (2025) and Zhang et al. (2025).

#### References

Baudouin, L., Marx, S., & Tarbouriech, S. (2019). Event-triggered damping of a linear wave equation. *IFAC-PapersOnLine*, 52(2), 58–63.

Demir, C., Diagne, M., & Krstic, M. (2024). Periodic event-triggered boundary control of neuron growth with actuation at soma. In 2024 IEEE 63rd conference on decision and control (pp. 434–439). IEEE.

Demir, C., Koga, S., & Krstic, M. (2024). Event-triggered control of neuron growth with actuation at soma. In 2024 American control conference (pp. 5301–5306).

Diagne, M., & Karafyllis, I. (2021). Event-triggered boundary control of a continuum model of highly re-entrant manufacturing systems. *Automatica*, 134, Article 109902.

Dolk, V., & Heemels, M. (2017). Event-triggered control systems under packet losses. Automatica, 80, 143–155.

Dolk, V. S., Ploeg, J., & Heemels, W. M. H. (2017). Event-triggered control for string-stable vehicle platooning. *IEEE Transactions on Intelligent Transportation Systems*, 18(12), 3486–3500.

Dolk, V. S., Tesi, P., De Persis, C., & Heemels, W. (2017). Event-triggered control systems under denial-of-service attacks. *IEEE Transactions on Control of Network Systems*, 4(1), 93–105.

Espitia, N. (2020). Observer-based event-triggered boundary control of a linear 2 × 2 hyperbolic systems. *Systems & Control Letters*. 138. Article 104668.

Espitia, N., Auriol, J., Yu, H., & Krstic, M. (2022a). Event-triggered output feedback control of traffic flow on cascaded roads. In Advances in distributed parameter systems (pp. 243–267). Springer.

Espitia, N., Auriol, J., Yu, H., & Krstic, M. (2022b). Traffic flow control on cascaded roads by event-triggered output feedback. *International Journal of Robust and Nonlinear Control*, 32(10), 5919–5949.

Espitia, N., Girard, A., Marchand, N., & Prieur, C. (2016). Event-based control of linear hyperbolic systems of conservation laws. *Automatica*, 70, 275–287.

Espitia, N., Karafyllis, I., & Krstic, M. (2021). Event-triggered boundary control of constant-parameter reaction-diffusion PDEs: A small-gain approach. *Automatica*, 128, Article 109562.

Espitia, N., Yu, H., & Krstic, M. (2020). Event-triggered varying speed limit control of stop-and-go traffic. *IFAC-PapersOnLine*, *53*(2), 7509–7514.

Kang, W., Baudouin, L., & Fridman, E. (2021). Event-triggered control of korteweg-de vries equation under averaged measurements. *Automatica*, 123, Article 109315.

Kang, W., Fridman, E., Zhang, J., & Liu, C.-X. (2023). Event-triggered stabilization of parabolic PDEs by switching. In 2023 62nd IEEE conference on decision and control (pp. 6899–6904). IEEE.

Katz, R., Fridman, E., & Selivanov, A. (2021). Boundary delayed observercontroller design for reaction-diffusion systems. *IEEE Transactions on Automatic Control*, 66(1), 275–282.

Koga, S., Demir, C., & Krstic, M. (2023). Event-triggered safe stabilizing boundary control for the stefan PDE system with actuator dynamics. In 2023 American control conference (pp. 1794–1799). IEEE.

Koudohode, F., Baudouin, L., & Tarbouriech, S. (2022a). Dynamic event-triggered stabilization for the Schrödinger equation. *IFAC-PapersOnLine*, 55(34), 120–125.

Koudohode, F., Baudouin, L., & Tarbouriech, S. (2022b). Event-based control of a damped linear wave equation. *Automatica*, 146, Article 110627.

Koudohode, F., Espitia, N., & Krstic, M. (2024). Event-triggered boundary control of an unstable reaction diffusion PDE with input delay. Systems & Control Letters, 186, Article 105775.

- Krstic, M., & Smyshlyaev, A. (2008). Boundary control of PDEs: A course on backstepping designs. SIAM.
- Lhachemi, H. (2024). Event-triggered finite-dimensional observer-based output feedback stabilization of reaction-diffusion PDEs. IEEE Transactions on Automatic Control.
- Rathnayake, B., & Diagne, M. (2022). Event-based boundary control of one-phase stefan problem: A static triggering approach. In *2022 American control conference* (pp. 2403–2408). IEEE.
- Rathnayake, B., & Diagne, M. (2023). Observer-based periodic event-triggered boundary control of the one-phase Stefan problem. *IFAC-PapersOnLine*, 56(2), 11415–11422.
- Rathnayake, B., & Diagne, M. (2024a). Observer-based event-triggered boundary control of the one-phase Stefan problem. *International Journal of Control*, 1–12.
- Rathnayake, B., & Diagne, M. (2024b). Observer-based periodic event-triggered and self-triggered boundary control of a class of parabolic PDEs. *IEEE Transactions on Automatic Control*.
- Rathnayake, B., Diagne, M., Cortés, J., & Krstic, M. (2025). Performance-barrier event-triggered control of a class of reaction-diffusion PDEs. Automatica, 174, Article 112181.
- Rathnayake, B., Diagne, M., Espitia, N., & Karafyllis, I. (2022). Observer-based event-triggered boundary control of a class of reaction-diffusion PDEs. *IEEE Transactions on Automatic Control*, 67(6), 2905–2917.
- Rathnayake, B., Diagne, M., & Karafyllis, I. (2022). Sampled-data and event-triggered boundary control of a class of reaction–diffusion PDEs with collocated sensing and actuation. *Automatica*, 137, Article 110026.
- Selivanov, A., & Fridman, E. (2016). Distributed event-triggered control of diffusion semilinear PDEs. Automatica, 68, 344–351.
- Somathilake, E., Rathnayake, B., & Diagne, M. (2024). Output feedback periodicevent and self-triggered control of coupled  $2\times 2$  linear hyperbolic PDEs. arXiv preprint arXiv:2404.02298.
- Triggiani, R. (1980). Boundary feedback stabilizability of parabolic equations. *Applied Mathematics and Optimization*, 6(1), 201–220.
- Vazquez, R., Krstic, M., & Coron, J.-M. (2011). Backstepping boundary stabilization and state estimation of a 2× 2 linear hyperbolic system. In 2011 50th IEEE conference on decision and control and European control conference (pp. 4937–4942). IEEE.
- Wakaiki, M., & Sano, H. (2019). Stability analysis of infinite-dimensional eventtriggered and self-triggered control systems with Lipschitz perturbations. arXiv preprint arXiv:1911.12916.
- Wakaiki, M., & Sano, H. (2020). Event-triggered control of infinite-dimensional systems. SIAM Journal on Control and Optimization, 58(2), 605–635.
- Wang, J., & Krstic, M. (2021). Adaptive event-triggered PDE control for load-moving cable systems. Automatica, 129, Article 109637.
- Wang, J., & Krstic, M. (2022a). Delay-compensated event-triggered boundary control of hyperbolic PDEs for deep-sea construction. *Automatica*, 138, Article

- Wang, J., & Krstic, M. (2022b). Event-triggered adaptive control of coupled hyperbolic PDEs with piecewise-constant inputs and identification. *IEEE Transactions on Automatic Control*, 68(3), 1568–1583.
- Wang, J., & Krstic, M. (2022c). Event-triggered output-feedback backstepping control of sandwich hyperbolic PDE systems. *IEEE Transactions on Automatic Control*, 67(1), 220–235.
- Wang, J., & Krstic, M. (2023). Event-triggered adaptive control of a parabolic PDE-ODE cascade with piecewise-constant inputs and identification. *IEEE Transactions on Automatic Control*, 68(9), 5493–5508.
- Yu, H., & Krstic, M. (2022). Traffic congestion control by PDE backstepping. Springer.
- Zhang, P., Rathnayake, B., Diagne, M., & Krstic, M. (2025). Performance-barrier event-triggered PDE control of traffic flow. (pp. 5720–5735).
- Zhang, Y., & Yu, H. (2024). Event-triggered boundary control of mixed-autonomy traffic. In 2024 IEEE 63rd conference on decision and control (pp. 6428–6433).



Bhathiya Rathnayake received his B.Sc. in Engineering, specializing in Electrical and Electronic Engineering, from the University of Peradeniya, Sri Lanka, in 2017. He earned his M.S. degree in Computer and Systems Engineering from Rensselaer Polytechnic Institute, New York, USA, in 2022. He obtained his Ph.D. degree in Electrical Engineering (Robotics, Intelligent Systems, and Control) from UC San Diego, California, USA, in 2025. Currently he is working as a Postdoctoral Fellow at Johns Hopkins University, Baltimore, USA. His research interests include control of infinite dimensional

systems, event-triggered control, and control of inverter-dominated power systems.



Mamadou Diagne is an Associate Professor with the Department of Mechanical and Aerospace Engineering at the University of California San Diego, affiliated with the Department of Electrical and Computer Engineering. He completed his Ph.D. inAutomatic Control in 2013 at University Claude Bernard Lyon I, Villeurbanne (France). Between 2017 and 2022, he was an Assistant Professor with the Department of Mechanical Aerospace and Nuclear Engineering at Rensselaer Polytechnic Institute, Troy, New York. From 2013 to 2016, he was a Postdoctoral Scholar, first at the University

of California San Diego, and then at the University of Michigan. His research focuses on the control of distributed parameter systems (DPS), adaptive control, time-delay systems, extremum seeking control and safe nonlinear control. He served as Associate Editor for Automatica, Systems & Control Letters and ASME Journal of Dynamic Systems, Measurement, and Control. He is Vice-Chair for Industry of the IFAC Technical Committee on Adaptive and Learning Systems and Vice-Chair for Education of the IFAC Technical Committee on Distributed Parameter Systems. He received the NSF Career Award in 2020.